GEM and other charge multipliers with VLSI pixel read-out

Ronaldo Bellazzini
INFN - Pisa

Table 1 Physical characteristics and performances of the micro-pattern detector

	Present prototype (2–10 keV)	Improved configuration (3.5–10 keV)
Drift/absorption gap	6 mm	30 mm
Drift field	3,000 V cm^{-1}	1,500 V cm^{-1}
Gas filling and pressure	(Ne 80%–DME 20%); 1 atm	(Ne 40%–DME 60%); 4 atm
Gas grain	5,000	2,500
Transverse diffusion in drift	80 μm	<100 μm
GEM thickness		…kapton foil
GEM hole geometry		…-μm pitch
GEM voltage		
Detection efficiency at 5.4 keV		
Read-out pixel size		
Number of pixels		
Read-out plane technology		
Track length/pixel size (6 keV)		…= 10%
Sensitivity to Her X1		…P = 1%
Sensitivity to 3C-273		…P = 1%
Sensitivity to MCG-6-30-15		
Gain in the integration time over SXRP (strong sources)		…C (over Bragg)
Gain in the integration time over SXRP (faint sources)		…00 (over Bragg)

We show also the observing time needed to measure (at 99% … micro-pattern gas chamber (MPGC) is placed at the focus of th… use only photons above 3.5 keV to compute the sensitivity. … modulation. Her X-1 is a galactic … polarimetry, a direct measure of … Seyfert-1 galaxy for which a broa… polarimeter foreseen in a future X… polarization of Thomson scattering… multiplier. VLSI, very large scale i… …ical sources if the …proved design we …antly reduces the …d, by …is a …sitive …e on …tron

letters to nature

…bility of a new generation of photoelectric polarimeters in the 2–10 keV band. The device can simultaneously also produce good images (50–100 μm), moderately good spectroscopy (16% full-width at half-maximum, at 5.4 keV), and fast, high-rate timing down to 150 eV. Moreover, being truly two-dimensional, it is non-dispersive and does not require rotation.

We also tested our capability to model the polarization detection processes. As absorption, slowing down, scattering and transverse diffusion of electrons in the drift are well known quantities, we may reliably predict the performance of another detector configuration that would be better optimized for astrophysical applications. It is based on an existing[31] VLSI (Very Large Scale Integration) readout chip combined with other well established detector technology. We can derive the polarimetric sensitivity of such detectors when installed at the focus of a real X-ray telescope. In Table 1 we compare the sensitivity of the present and final configuration of the MPGC with SXRP.

The MPGC requires integration periods that are about 100 times shorter than those of the SXRP to detect the same polarization in bright sources. With integrations of the order of one day we could perform polarimetry of active galactic nuclei at the 1% level, a breakthrough in this fascinating window of high-energy astrophy-

9. Connors, P. A. & Stark, R. F. Observable gravitational effects on polarized radiation coming from near a black hole. *Nature* 269, 128–129 (1977).
10. Stark, R. F. & Connors, P. A. Observational test for the existence of a rotating black hole in Cyg X-1. *Nature* 266, 429–430 (1977).
11. Connors, P. A., Piran, T. & Stark, R. Polarization features of X-ray radiation emitted near a black hole. *Astrophys. J.* 235, 224–244 (1980).
12. Bao, G., Wiita, P. & Hadrava, P. Energy-dependent polarization variability as a black hole signature. *Phys. Rev. Lett.* 77, 12–15 (1996).
13. Celotti, A. & Matt, G. Polarization properties of synchrotron self-Compton emission. *Mon. Not. R. Astron. Soc.* 268, 451–458 (1994).
14. Poutanen, J. Relativistic jets in blazars: polarization of radiation. *Astrophys. J. Suppl. Ser.* 92, 607–609 (1994).
15. Tanaka, Y. *et al.* Gravitationally redshifted emission implying an accretion disk and massive black-hole in the active galaxy MCG-6-30-15. *Nature* 375, 659–661 (1995).
16. Ogura, J., Nobuyori, O. & Kojima, Y. Profiles and polarization properties of emission lines from relativistic disks. *Publ. Astron. Soc. Jpn* 52, 841–845 (2000).
17. Matt, G., Fabian, A. C. & Ross, R. R. X-ray photoionized accretion discs: UV and X-ray continuum spectra and polarization. *Mon. Not. R. Astron. Soc.* 264, 839–852 (1993).
18. Novick, R., Weisskopf, M. C., Berthelsdorf, R., Linke, R. & Wolff, R. S. Detection of X-ray polarization of the Crab Nebula. *Astrophys. J.* 174, L1–L8 (1972).
19. Weisskopf, M. C., Silver, E. H., Kestenbaum, H. L., Long, K. S. & Novick, R. A precision measurement of the X-ray polarization of the Crab Nebula without pulsar contamination. *Astrophys. J.* 220, L117–L122 (1978).
20. Kaaret, P. *et al.* SXRP: a focal plane stellar X-ray polarimeter for the Spectrum-X-Gamma mission. *Opt. Eng.* 29, 773–783 (1990).
21. Schnopper, H. W. & Kalata, K. Polarimeter for celestial X-rays. *Astron. J.* 74, 854–858 (1969).
22. Novick, R. in *Planets, Stars and Nebulae Studied with Photopolarimetry* (ed. Gerehls, T.) 262–317 (Univ. Arizona Press, Tucson, 1972).

30. Sauli, F. GEM: a new concept for electron amplification in gas detectors. *Nucl. Instrum. Methods A* 386, 531–534 (1997).
31. Campbell, M. *et al.* A pixel readout chip for 10–30 Mrad in standard 0.25μm CMOS. *IEEE Trans. Nucl. Sci.* 46, 156–160 (1999).
32. Bavdaz, M. *et al.* Status of the X-ray evolving universe spectroscopy mission (XEUS). *Proc. SPIE* 4138, 69–78 (2000).
33. Christensen, F. E. *et al.* X-ray calibration of the SODART flight telescope. *Proc. SPIE* 3113, 69–78 (1997).

An efficient photoelectric X-ray polarimeter for the study of black holes and neutron stars

E. Costa, P. Soffitta, R. Bellazzini, A. Brez, N. Lumb, G. Spandre

Nature, Vol. 411 (2001) 662.

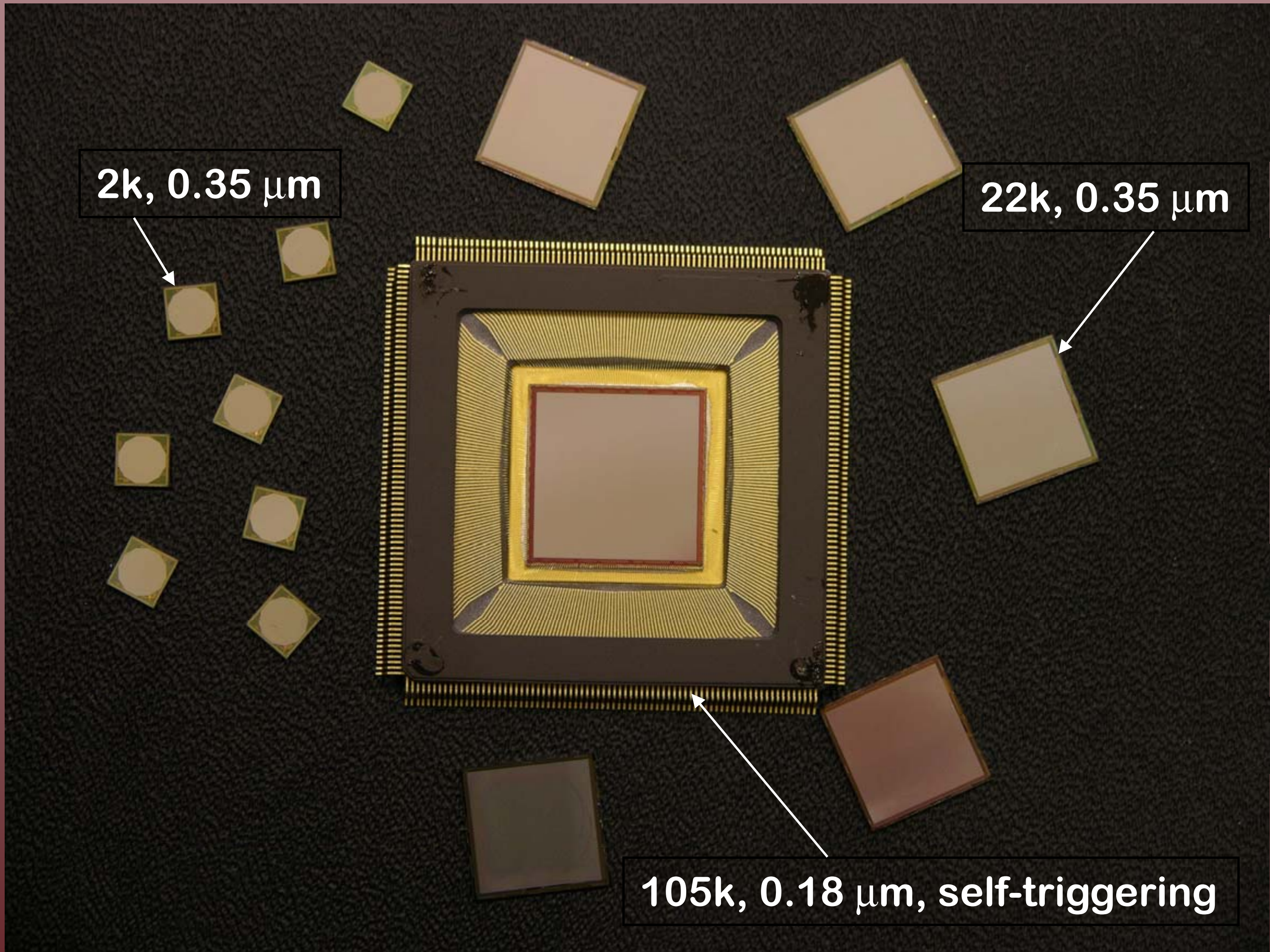

Three ASIC generations of increasing size, reduced pitch and improved functionality have been realized

The collecting anode/read-out VLSI chip

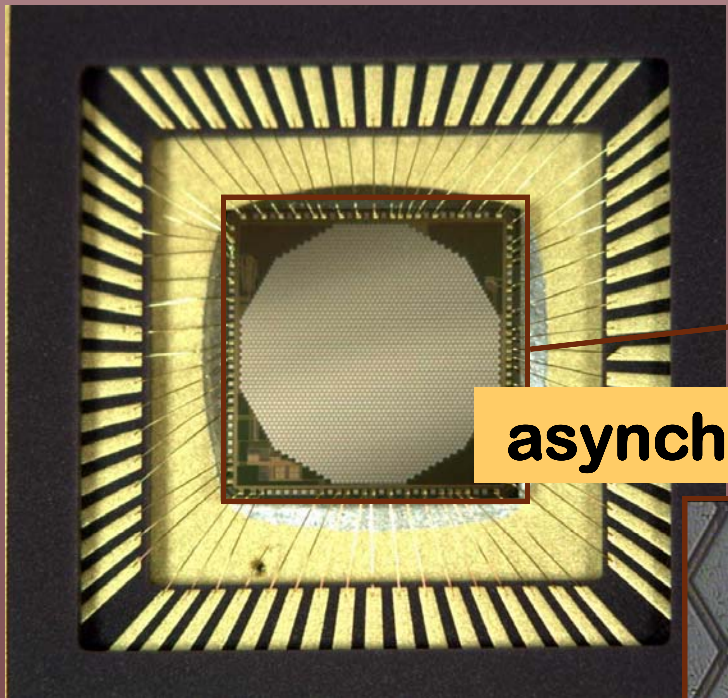

First ASIC prototype

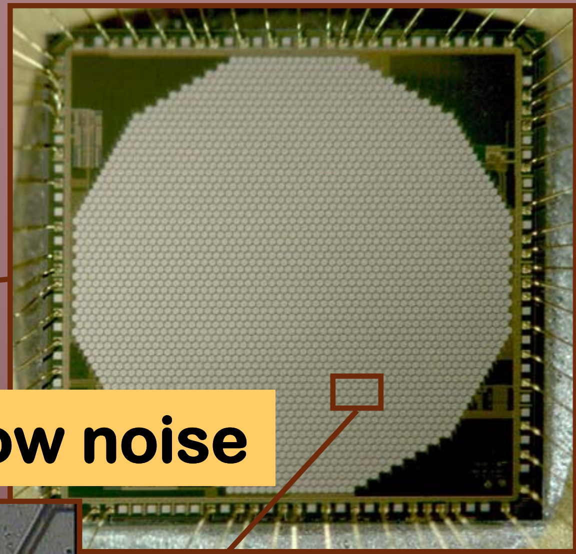

asynchronous, fast, low noise

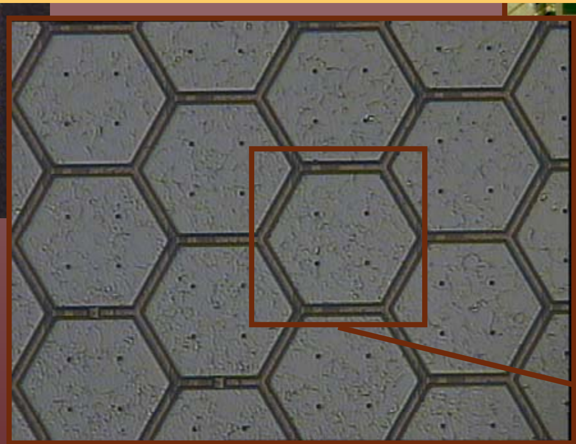

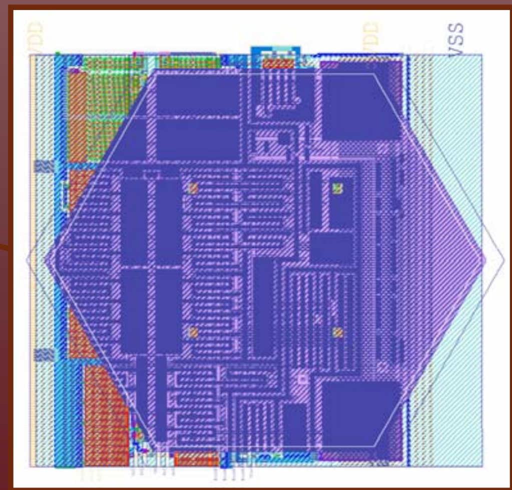

pixel electronics dimension:
80 μm x 80 μm in an hexagonal array,
comprehensive of preamplifier/shaper, S/H and routing (serial read-out) for each pixel
number of pixels: 2101

~3.5 μs shaping time
100 e- ENC
100 mv/fC input sensitivity
20 fC dynamic range

Last technological step:
a 0.18 μm CMOS VLSI

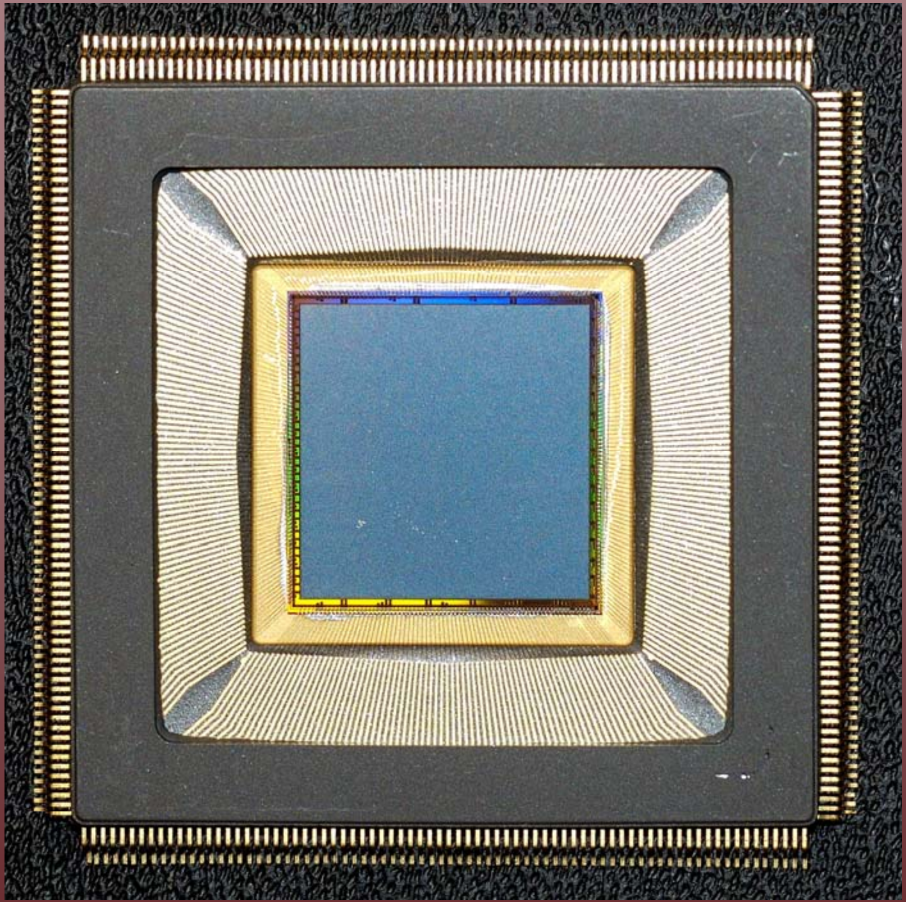

The chip integrates more than
16.5 million transistors.
It has a15mm x 15mm active area
of 105’600 pixels
organized in a honeycomb matrix

470 pixels/mm^2

Matrix organization

300 (width=300x50μm=15mm) x 352 (height=352x43.3μm=15.24mm) pixels
16 clusters of 300 x 22 = 6600 pixels each or
8 clusters of 300 x 44 = 13200 pixels each

0.18 μm ASIC features

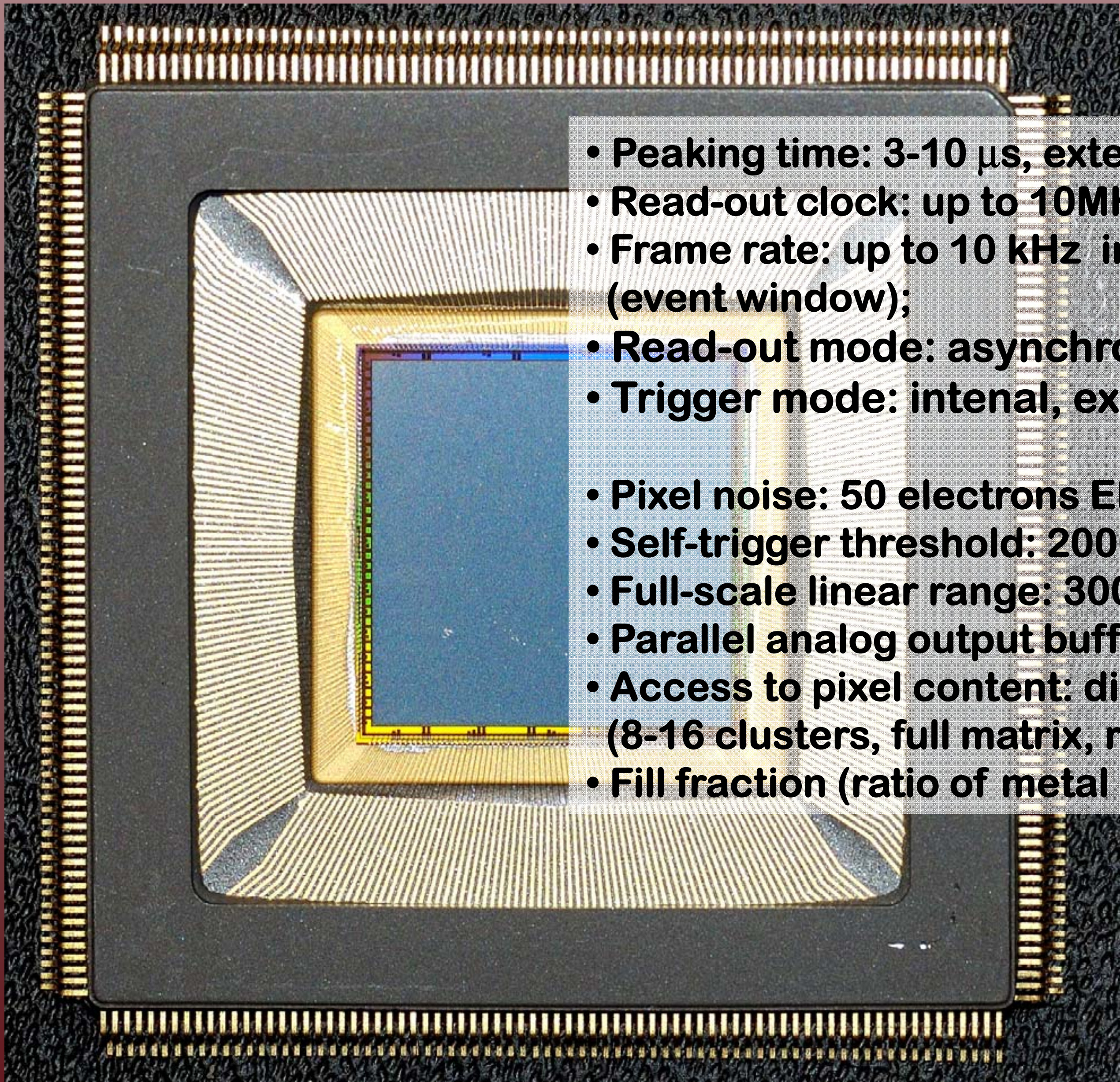

- Peaking time: 3-10 μs, externally adjustable;
- Read-out clock: up to 10MHz;
- Frame rate: up to 10 kHz in self-trigger mode (event window);
- Read-out mode: asynchronous or synchronous;
- Trigger mode: intenal, external or self-trigger;

- Pixel noise: 50 electrons ENC;
- Self-trigger threshold: 2000 electrons;
- Full-scale linear range: 30000 electrons;
- Parallel analog output buffers: 1, 8 or 16;
- Access to pixel content: direct (single pixel) or serial (8-16 clusters, full matrix, region of interest);
- Fill fraction (ratio of metal area to active area): 92%

Total power dissipation ~ 0.5 Watt

Detector assembly

- GEM pitch: 50 μm
- GEM holes diameters: 33 μm, 15 μm
- Read out pitch: 50 μm
- Absorption gap thickness: 10 mm
- Collection gap thickness: 1 mm

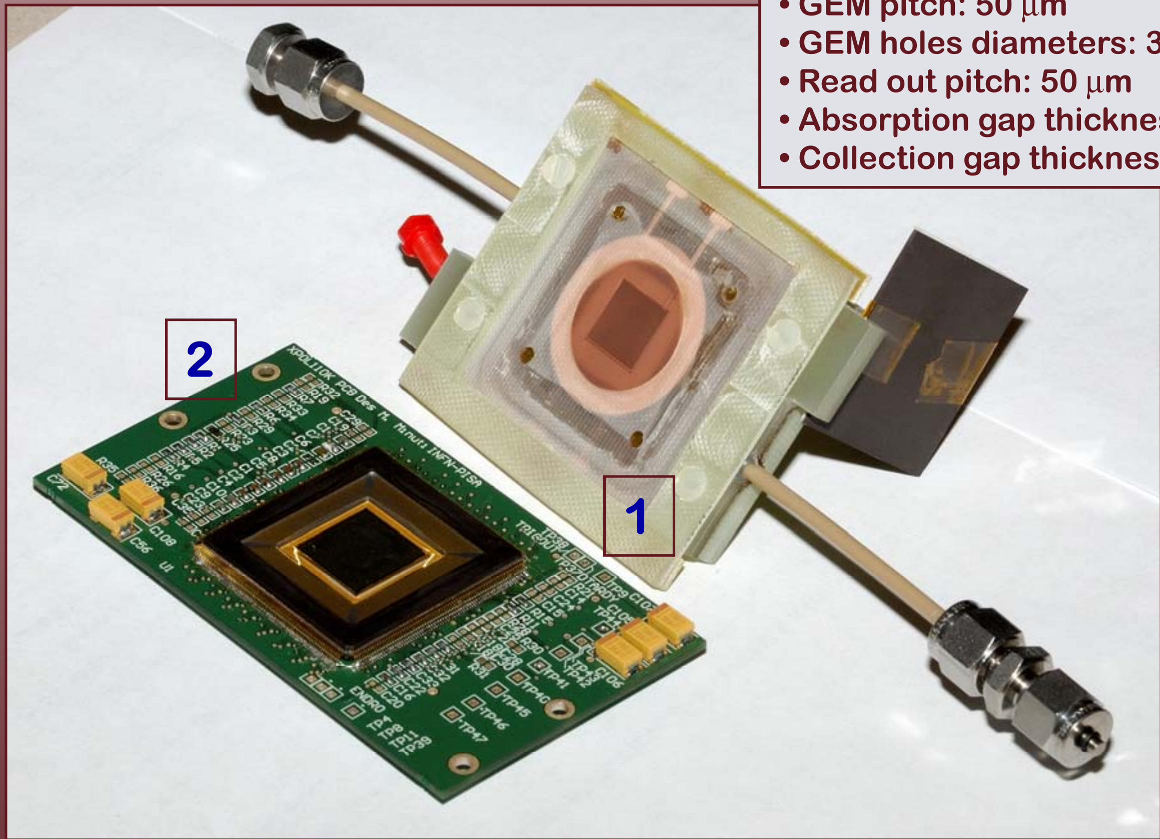

1 - The GEM glued to the bottom of the gas-tight enclosure
2 - The large area ASIC mounted on the control motherboard

Large effective gas gain around 1000 @450V in Ne(50%)-DME(50%)
(at least 70 V less than in our standard 90 μm pitch GEM)

GEM specs

pitch: 50 µm

holes inner Ø: 15 µm

holes outer Ø: 35 µm

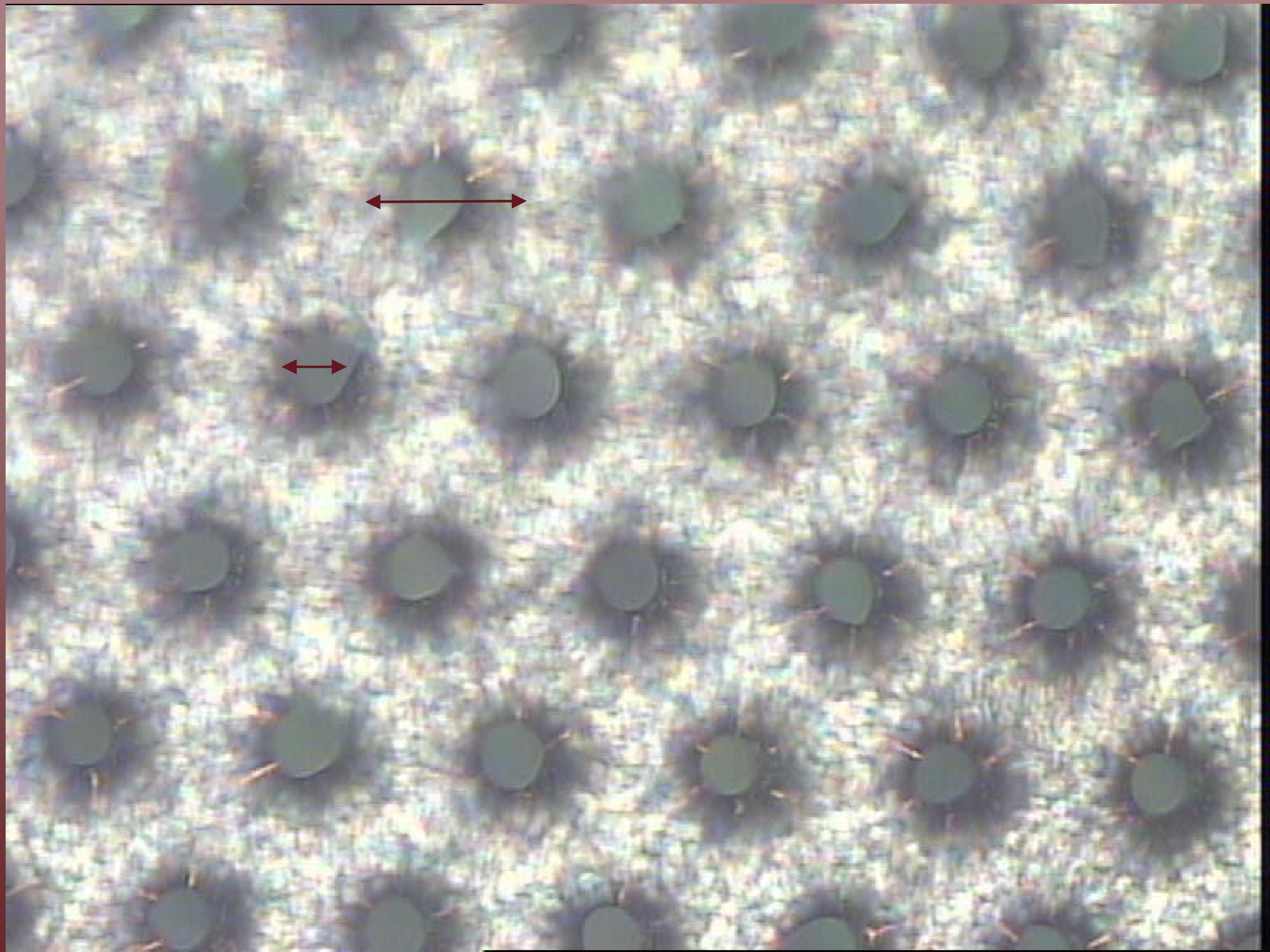

The matching of readout and gas amplification (GEM) pitch allows getting optimal results and to fully exploit the very high granularity of the device

Imaging capability

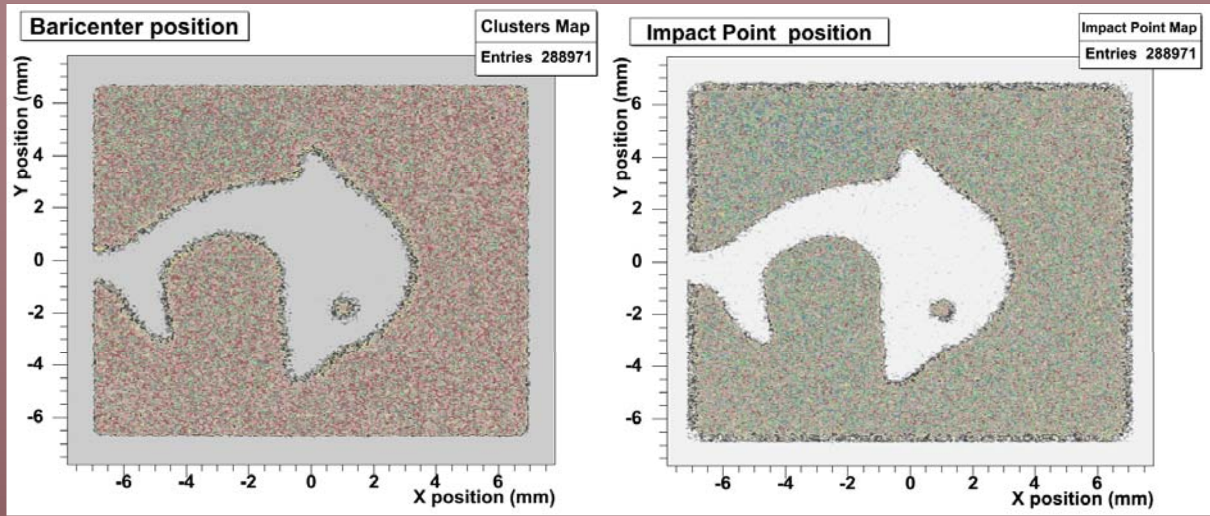

^{55}Fe source **Ne(50%)-DME(50%)**

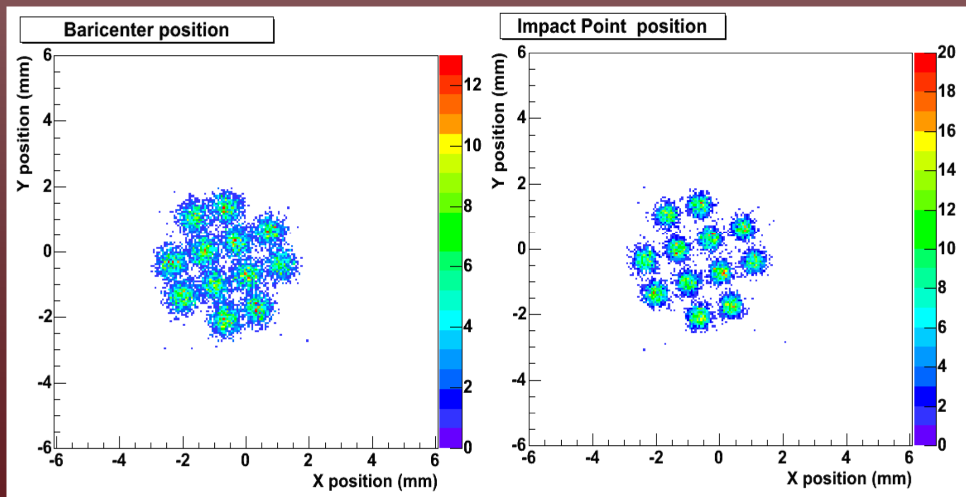

Holes: 0.6 mm diameter, 2 mm apart.

Imaging and spectroscopic capability

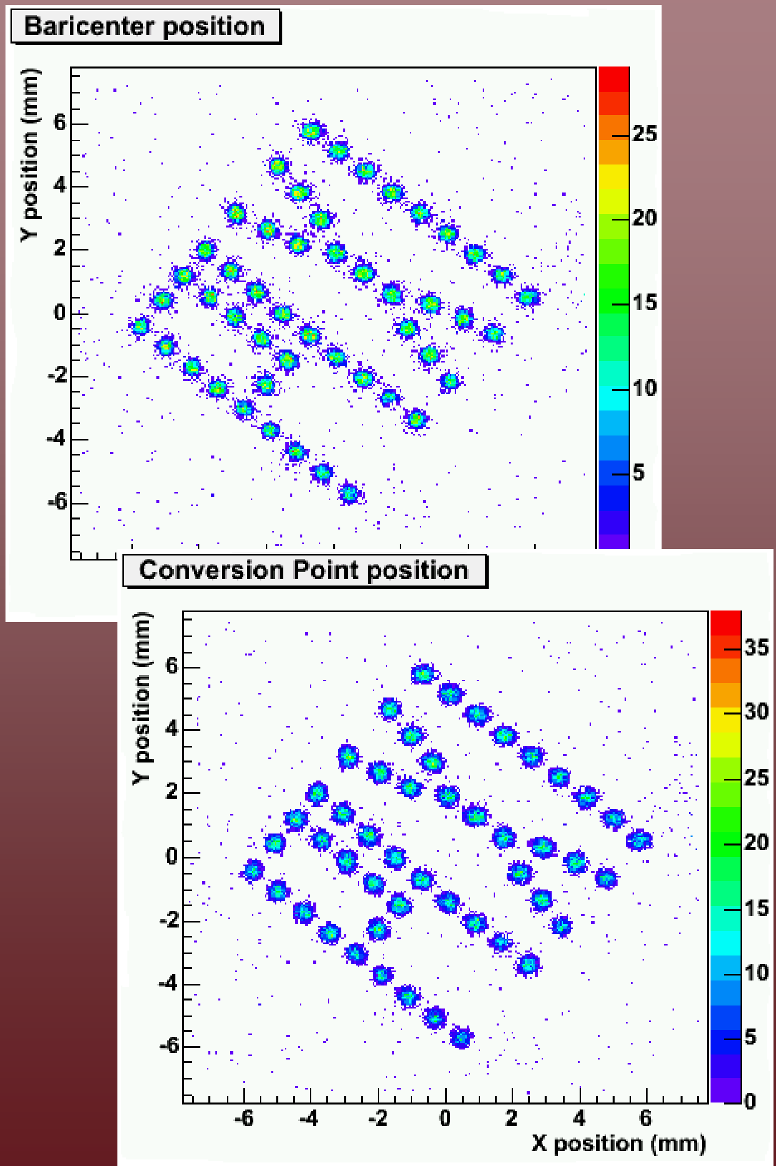

Argon (50%)-DME(50%)

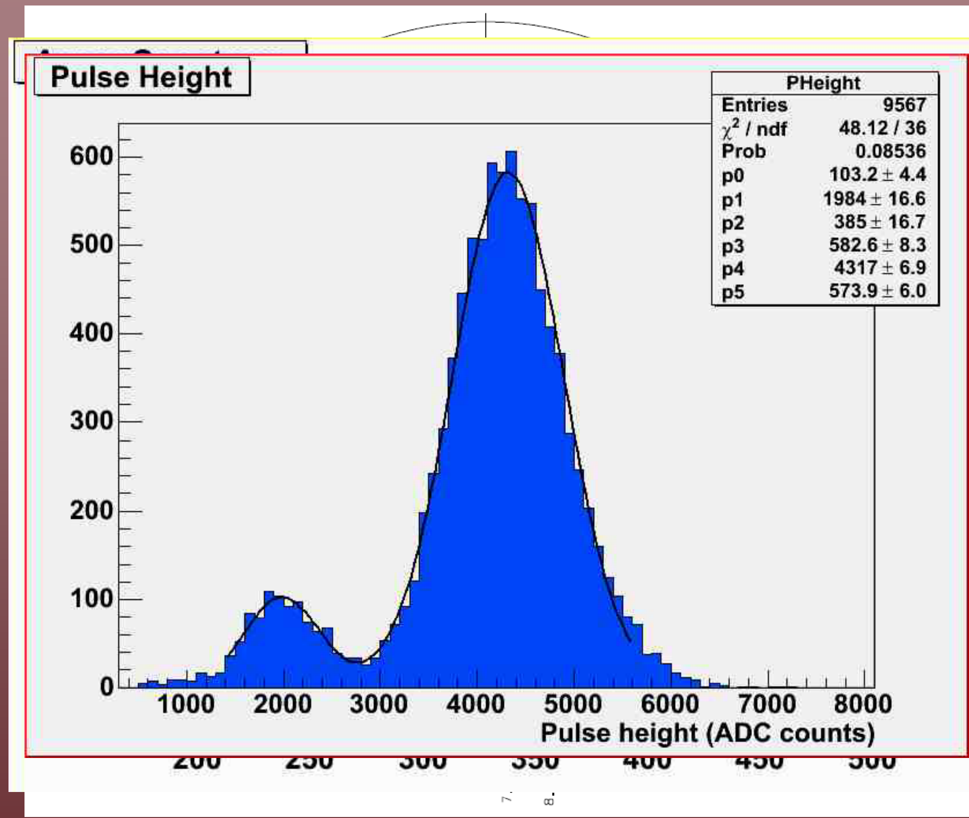

Holes:
Ø 0.5 mm
pitch 1 mm

Track morphology and angle reconstruction

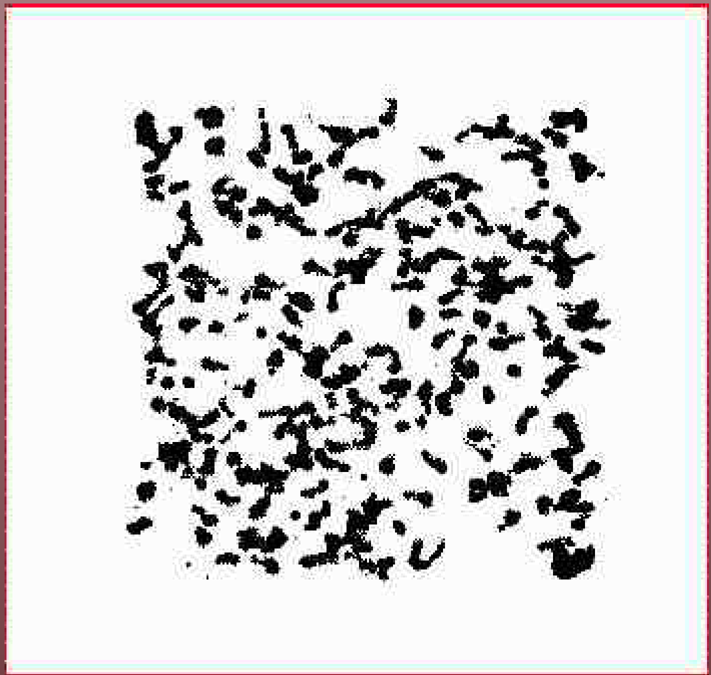

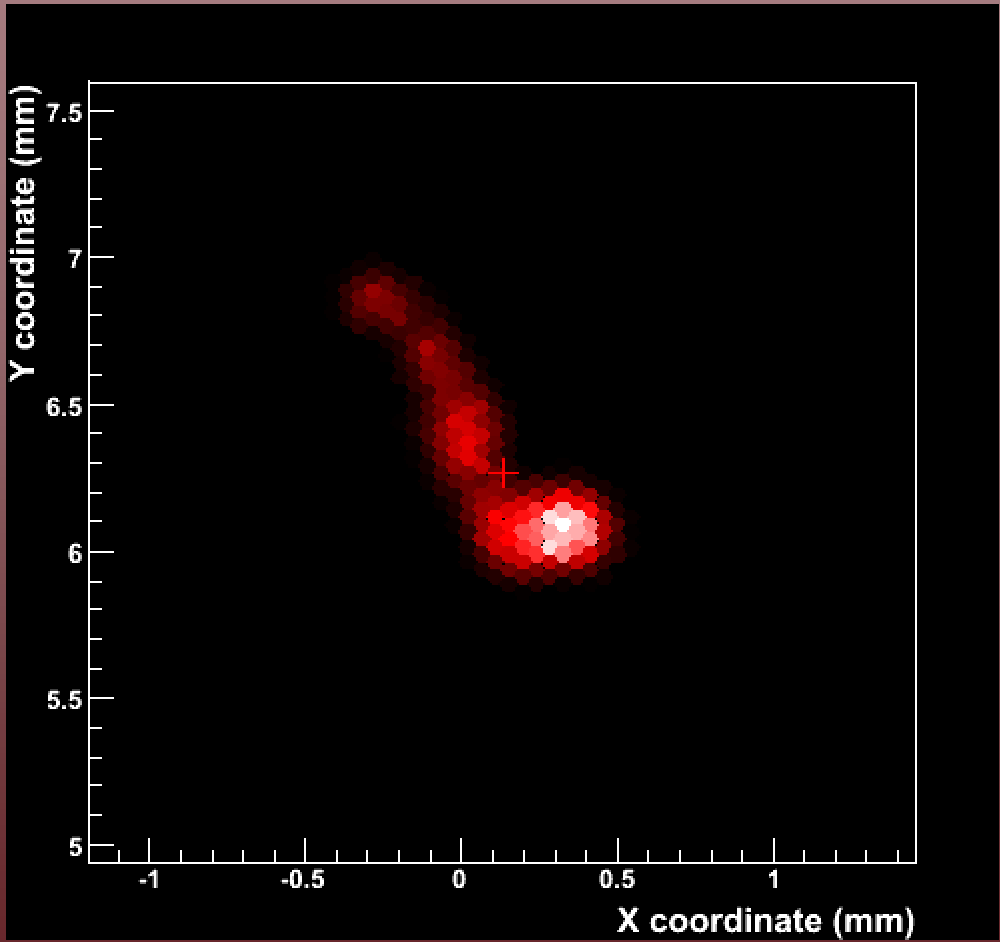

On-line monitoring

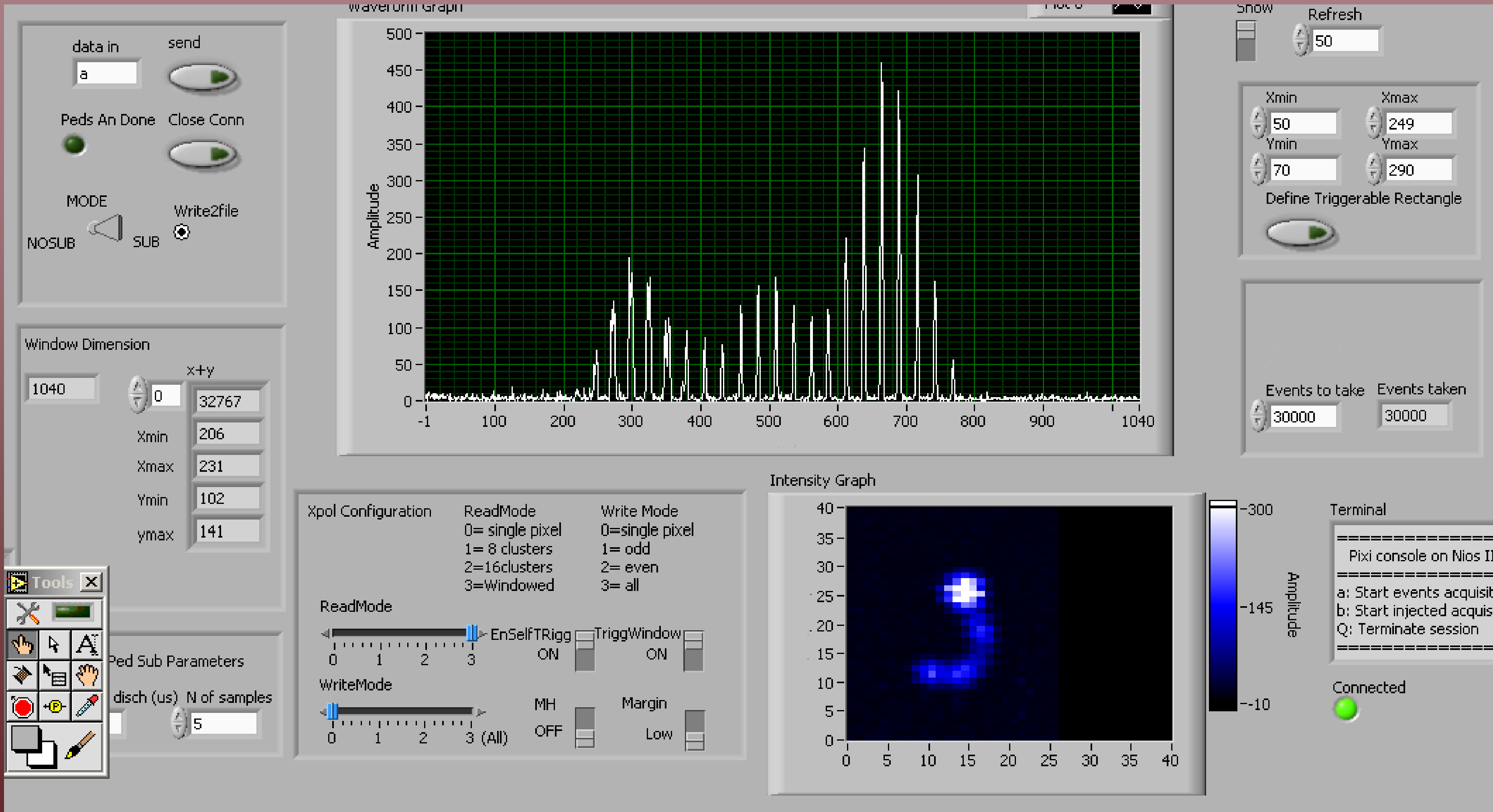

Real time pedestal subtraction

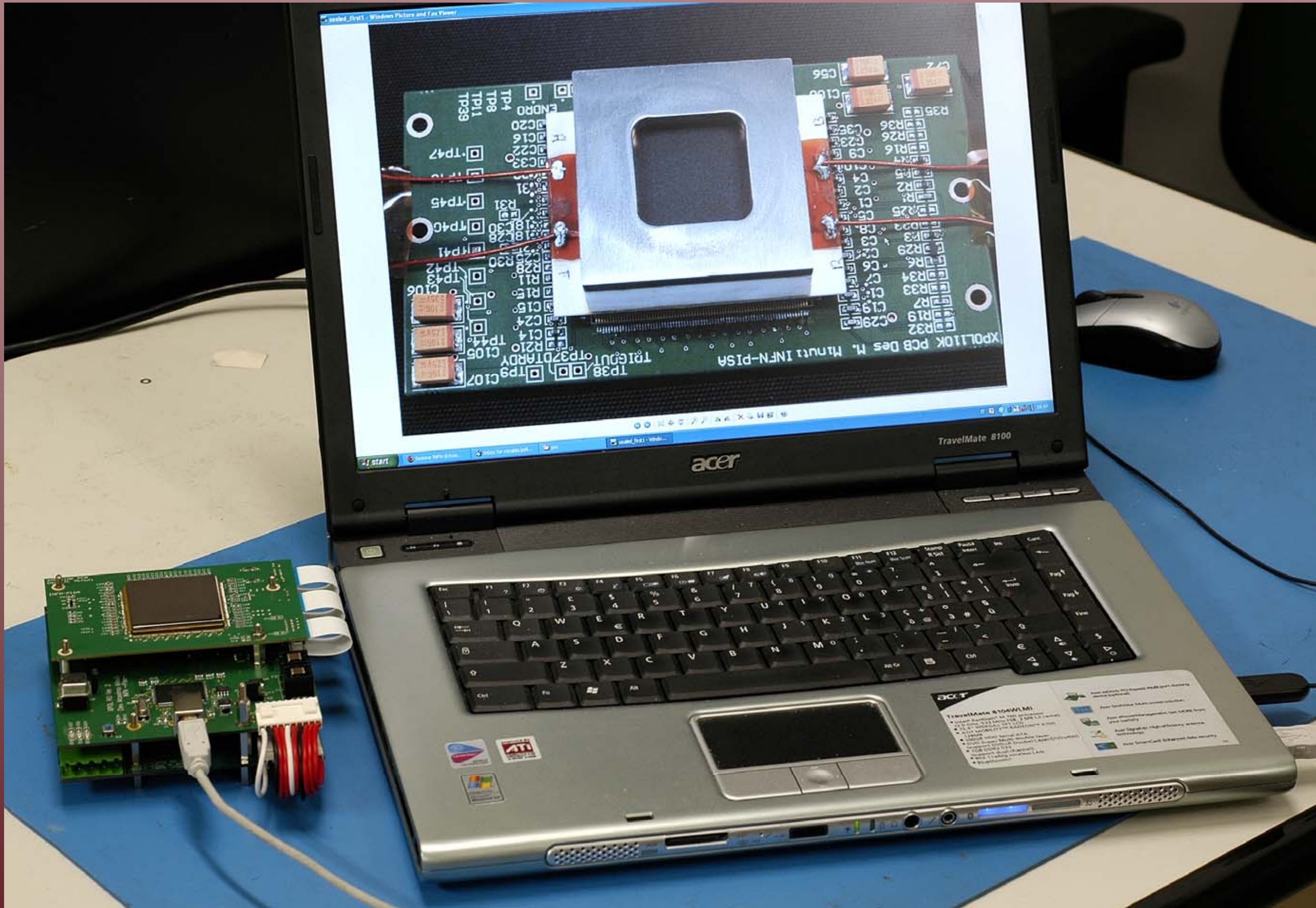

. The level of integration, compactness and operational simplicity of this device is comparable to solid state detectors

Sealed device
(only clean materials, baking & outgassing)

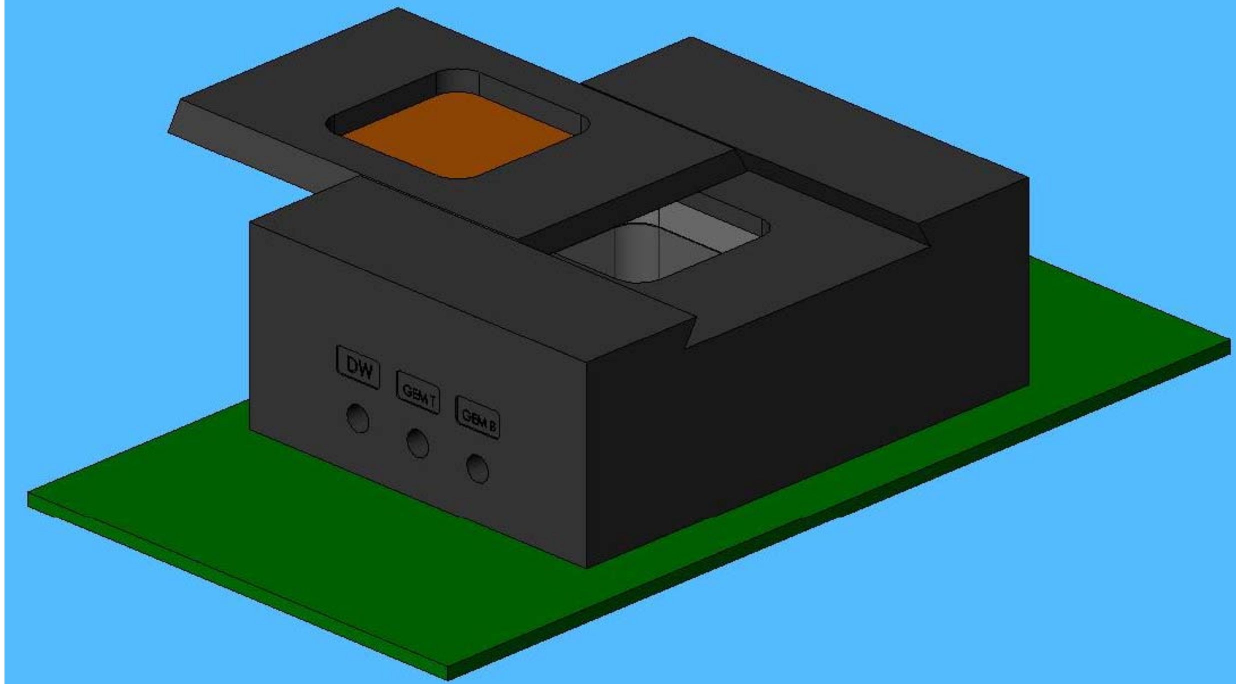

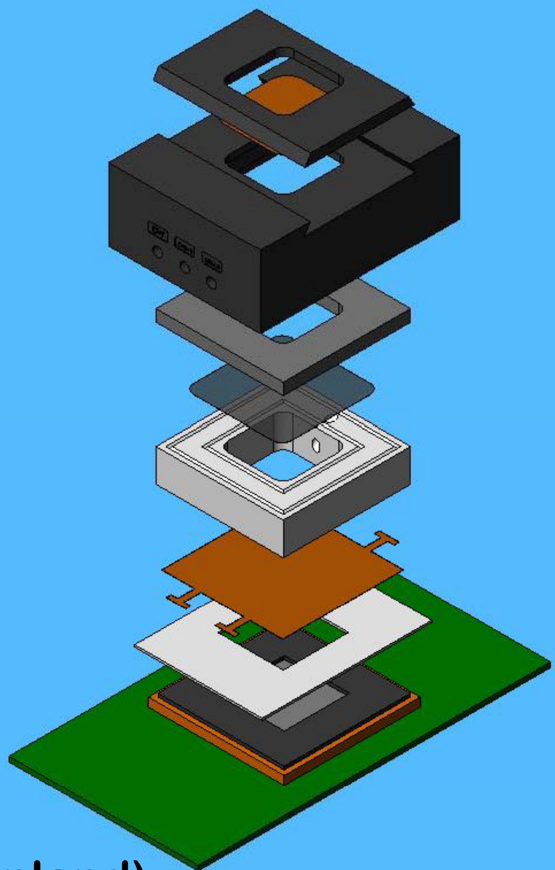

Collaboration with Oxford Instruments Analytical Oy (Finland)

Long-term gain stability

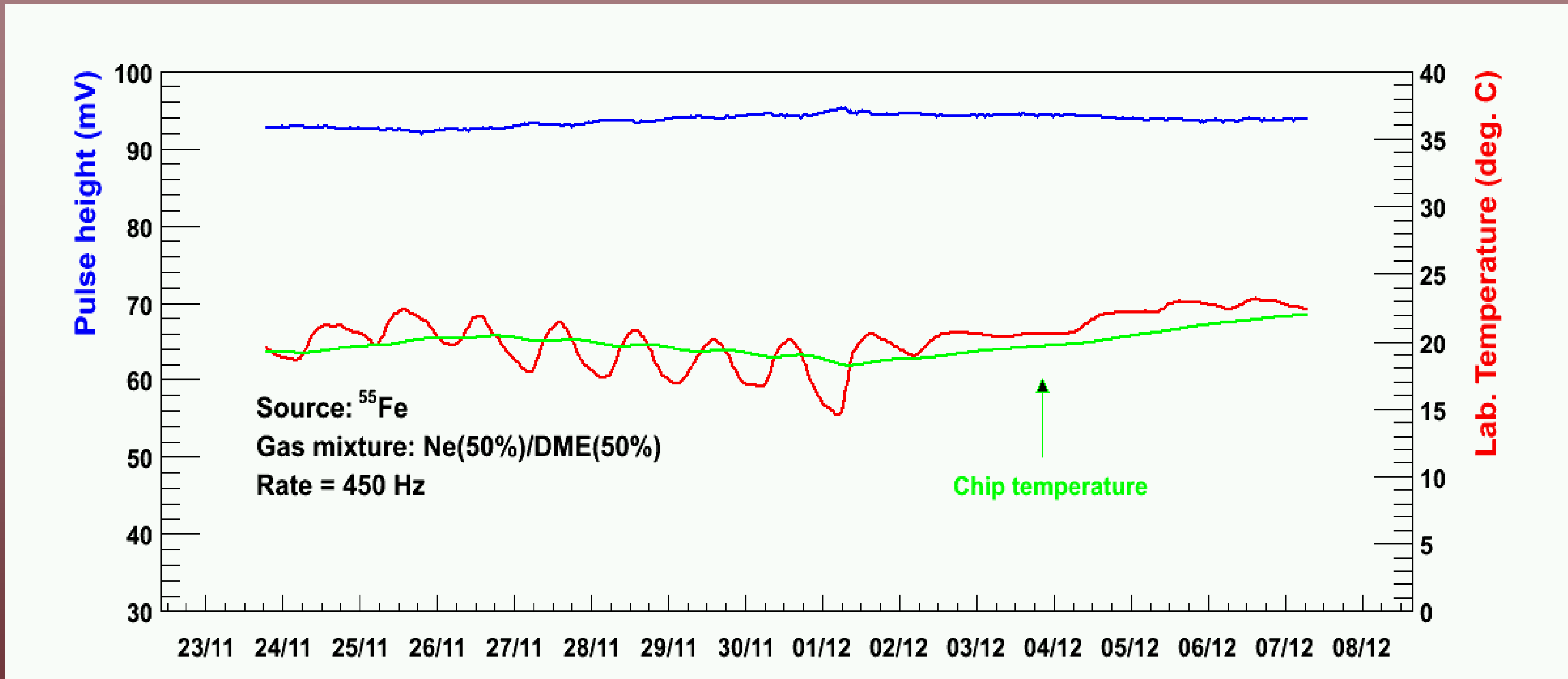

Irradiation with ^{55}Fe has started on November 20th
Pulse height registration on 23rd at 7:30pm.

Semitransparent Photocathode

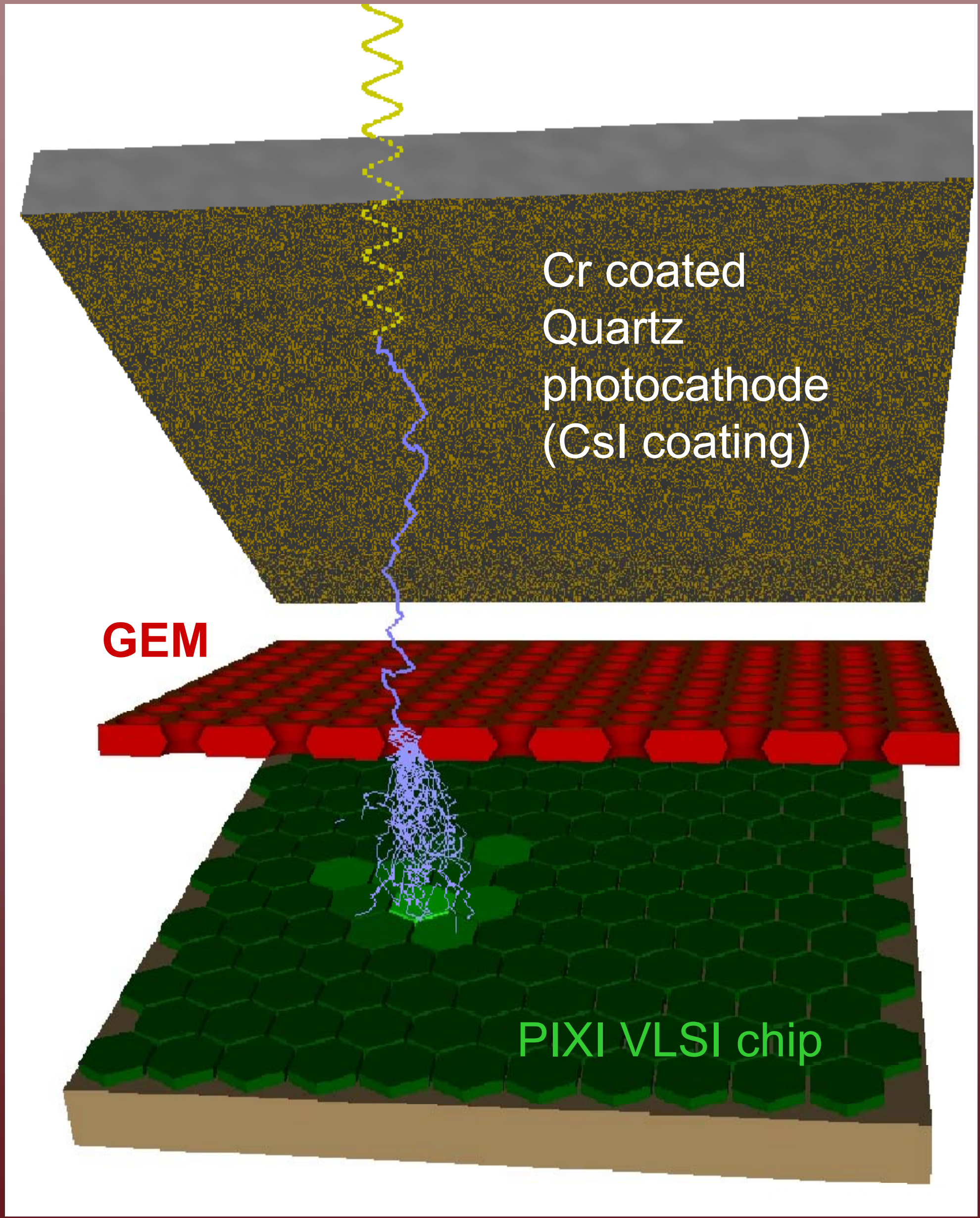

Drift gap = 1 mm
Transfer gap = 1mm
GEM thickness = 50 μm
GEM pitch = 50 μm

Pros:
- Simple
- High gain
- High geometrical efficiency

Cons:
- Low thickness → Low Q.E.
- Extra diffusion in the gas layer above the GEM

Reflective Photocathode

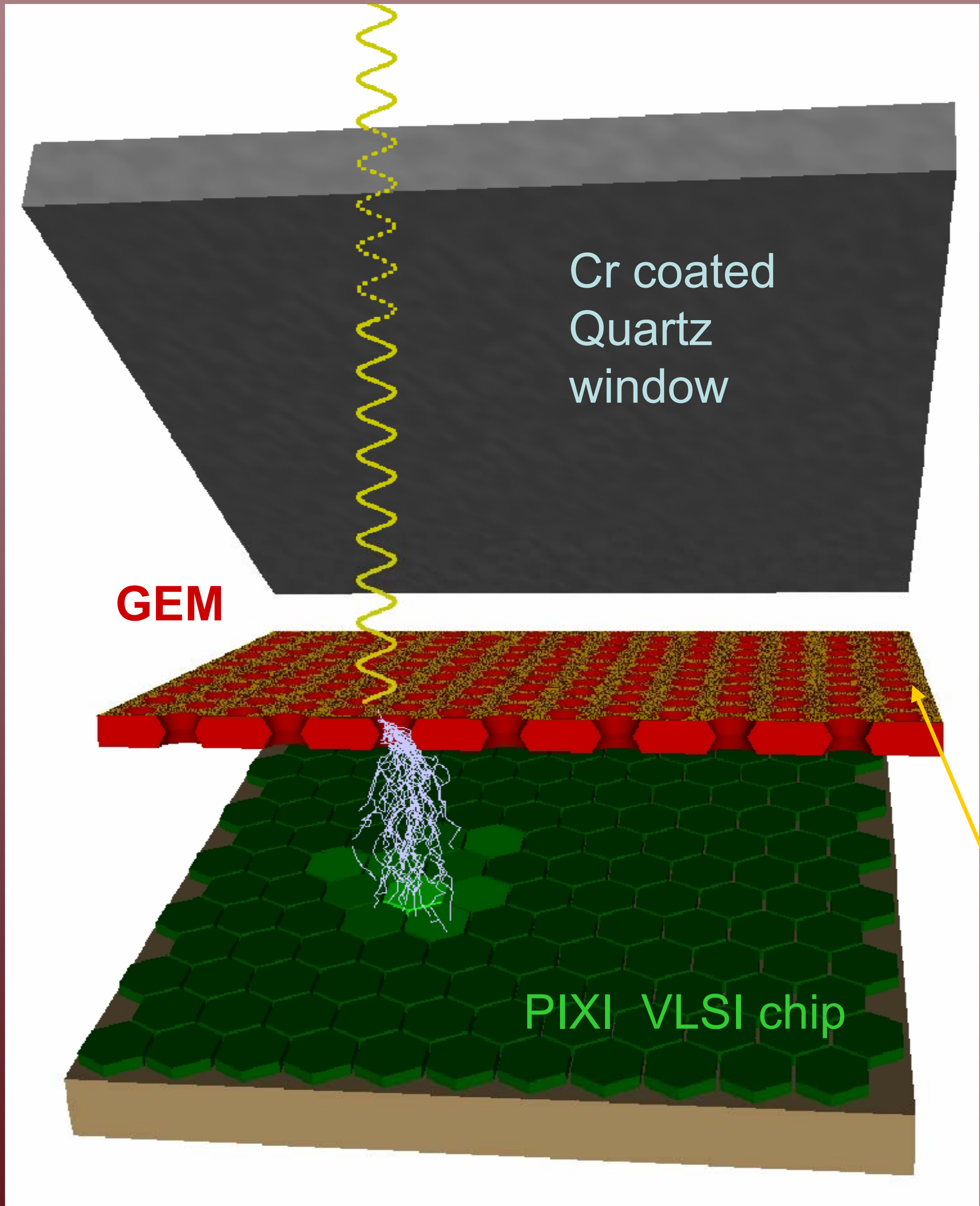

Drift gap = 1 mm
Transfer gap = 1mm
GEM thickness = 50 μm
GEM pitch = 50 μm

Pros:
- Thick film → high Q.E. (10-20%)

Cons:
- More complicated to build
- Special gold coating on the GEM
- Low geometrical efficiency (in our case 50%)
- Lower gas gain

CsI photocathode

UV photo-detector with *single electron* sensitivity

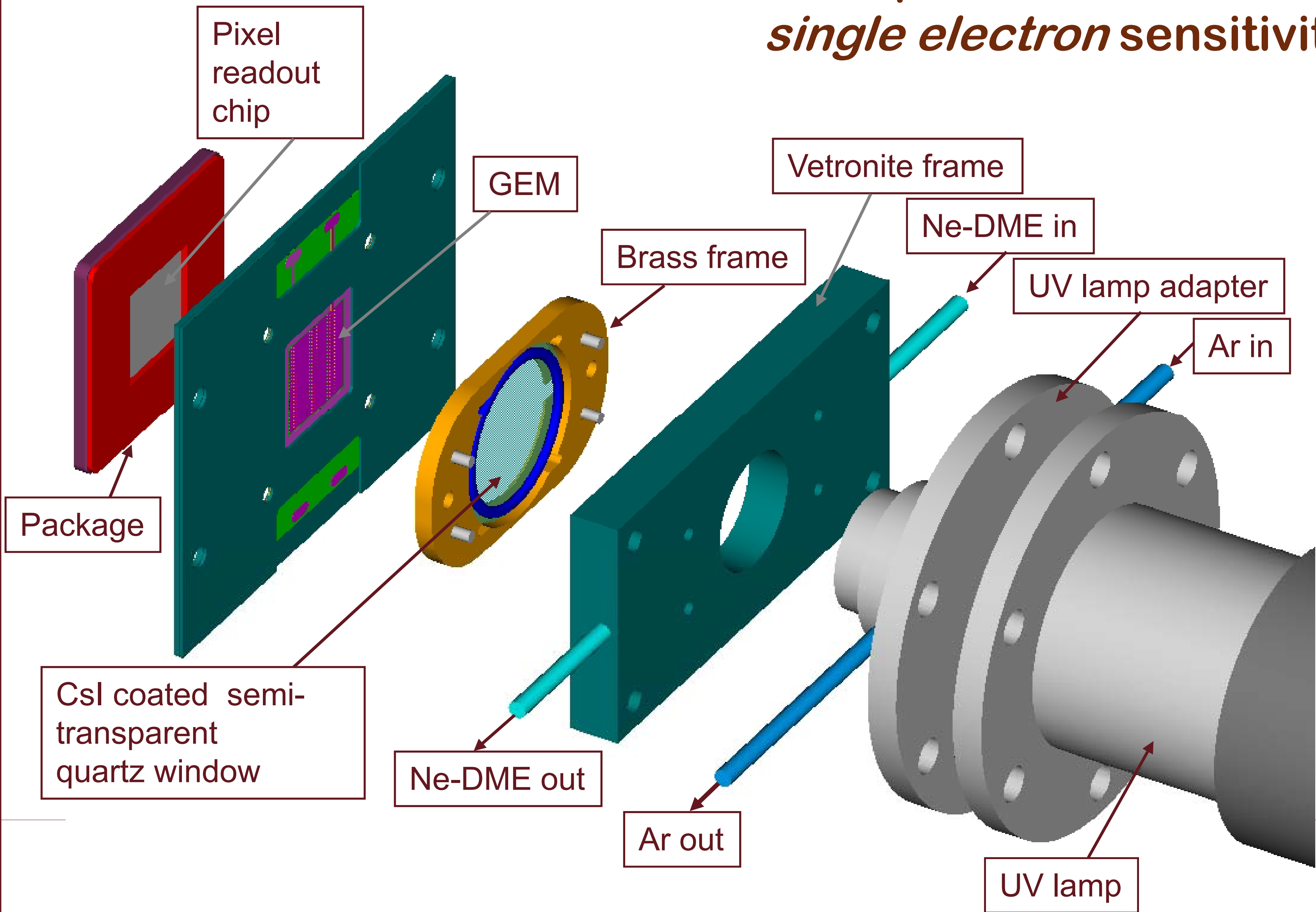

Single photon operation

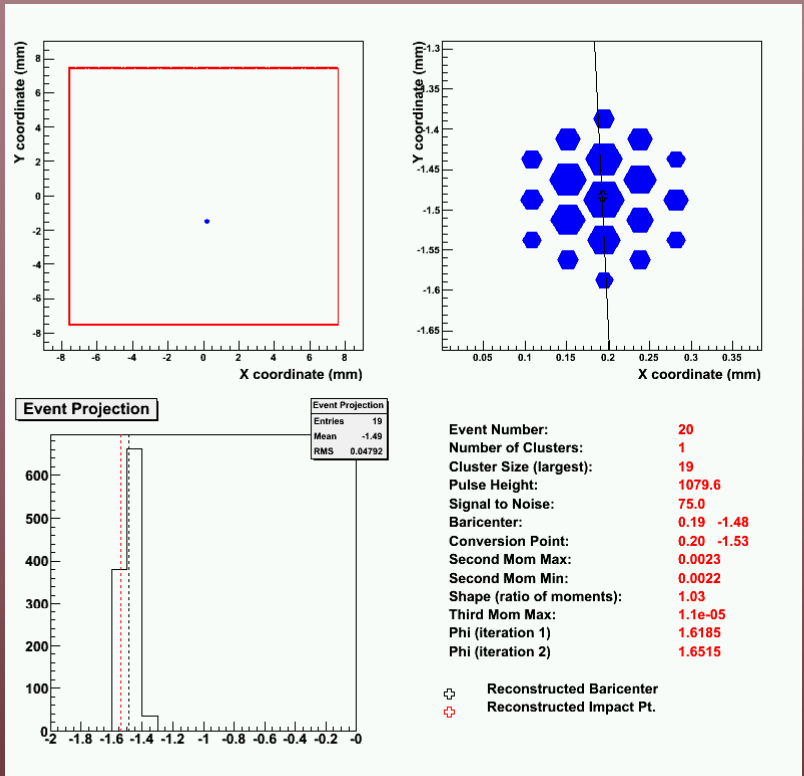

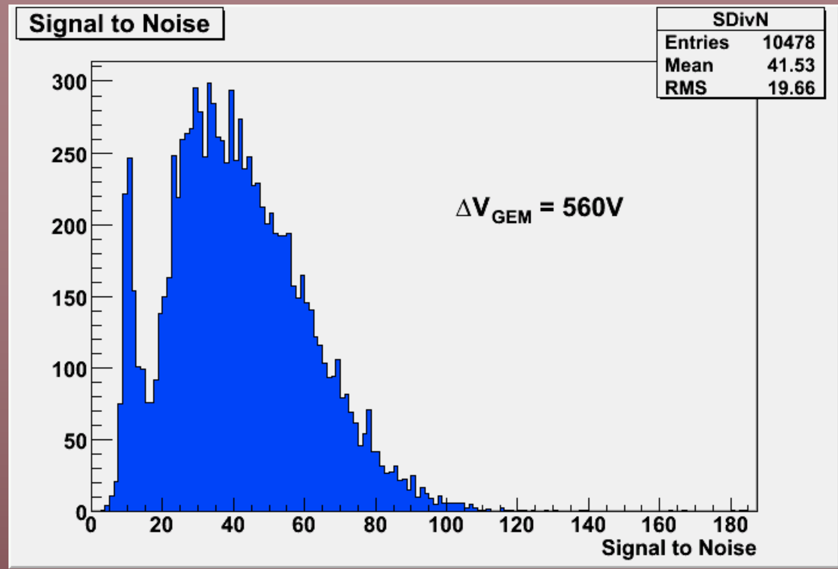

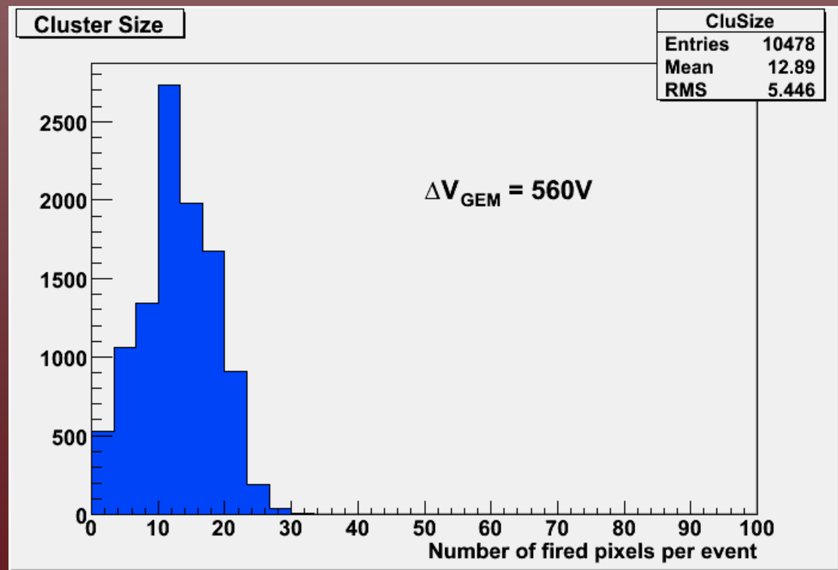

Single photon event topology

Semitransparent Photocathode

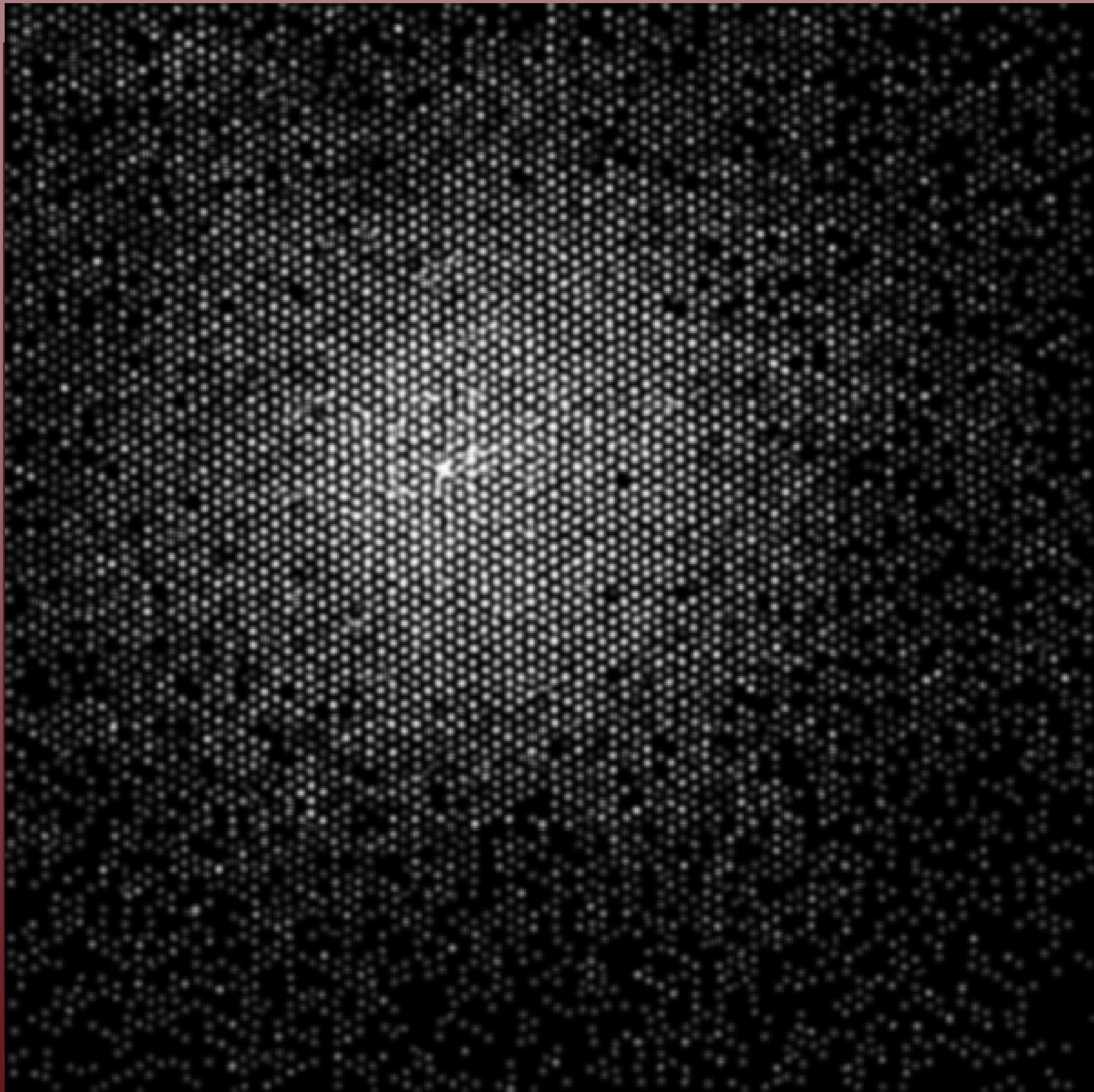

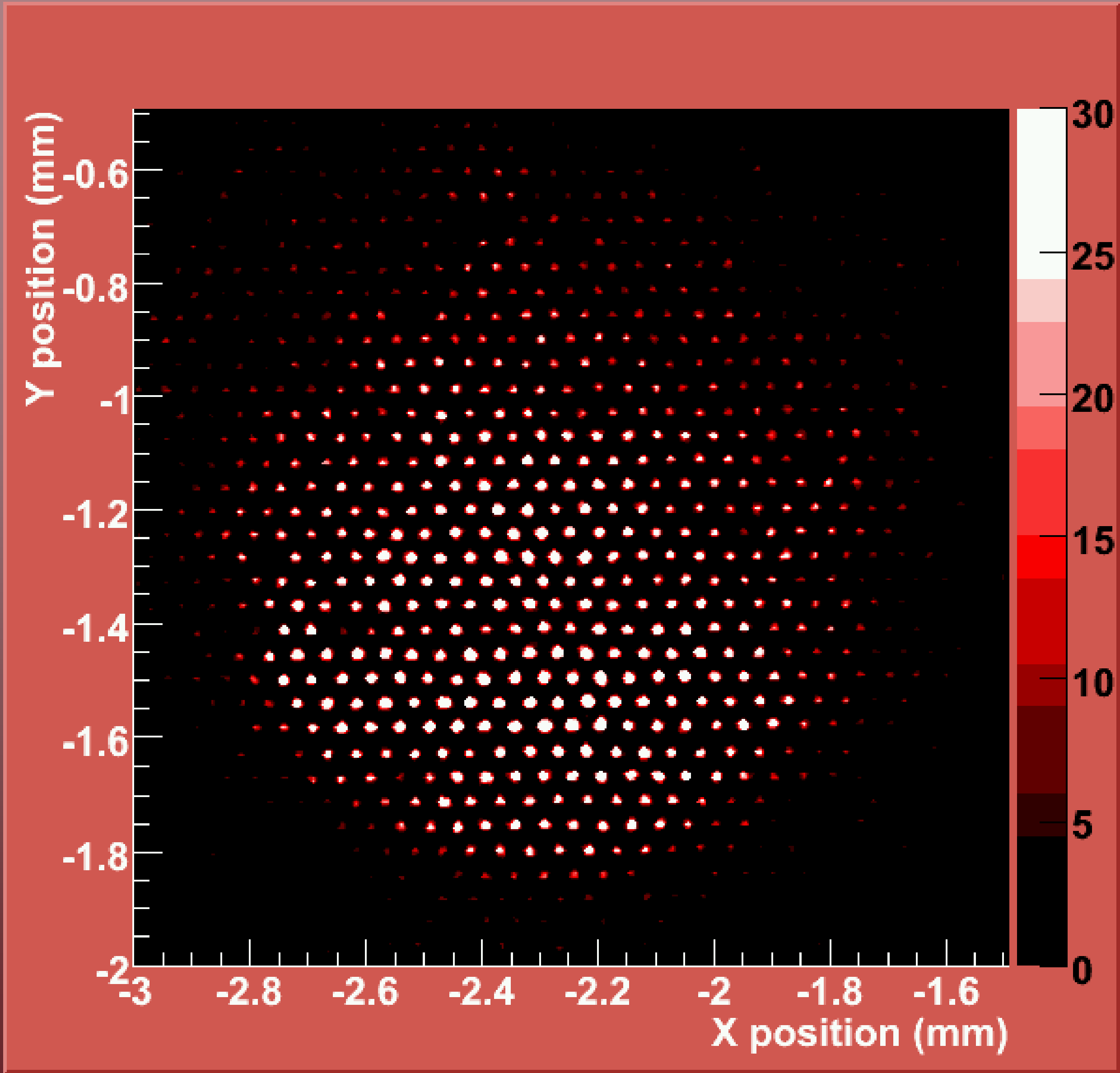

"Self-portrait" of the GEM amplification structure

Intrinsic resolution of the read-out system

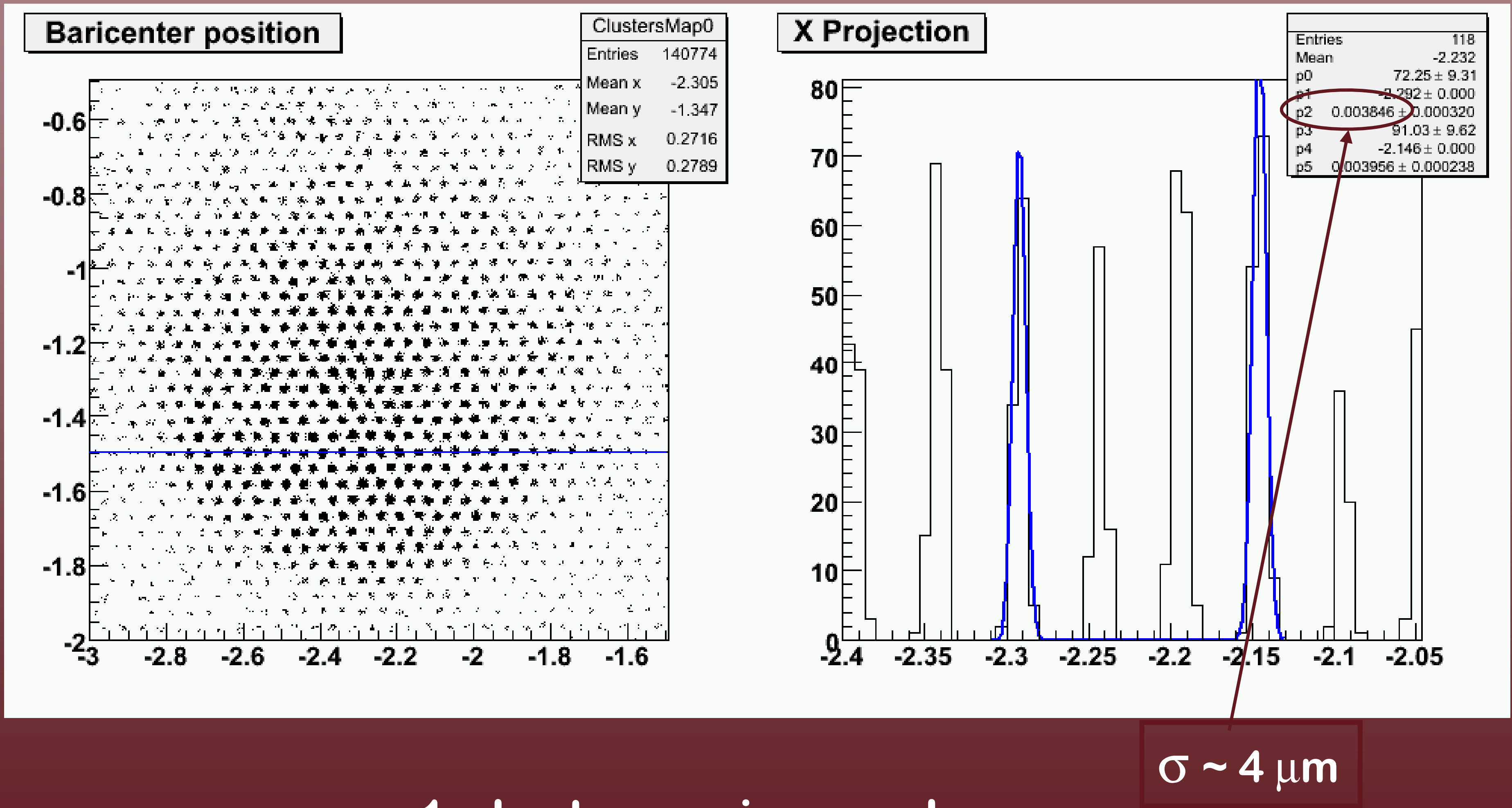

1 electron primary charge

Semitransparent Photocathode

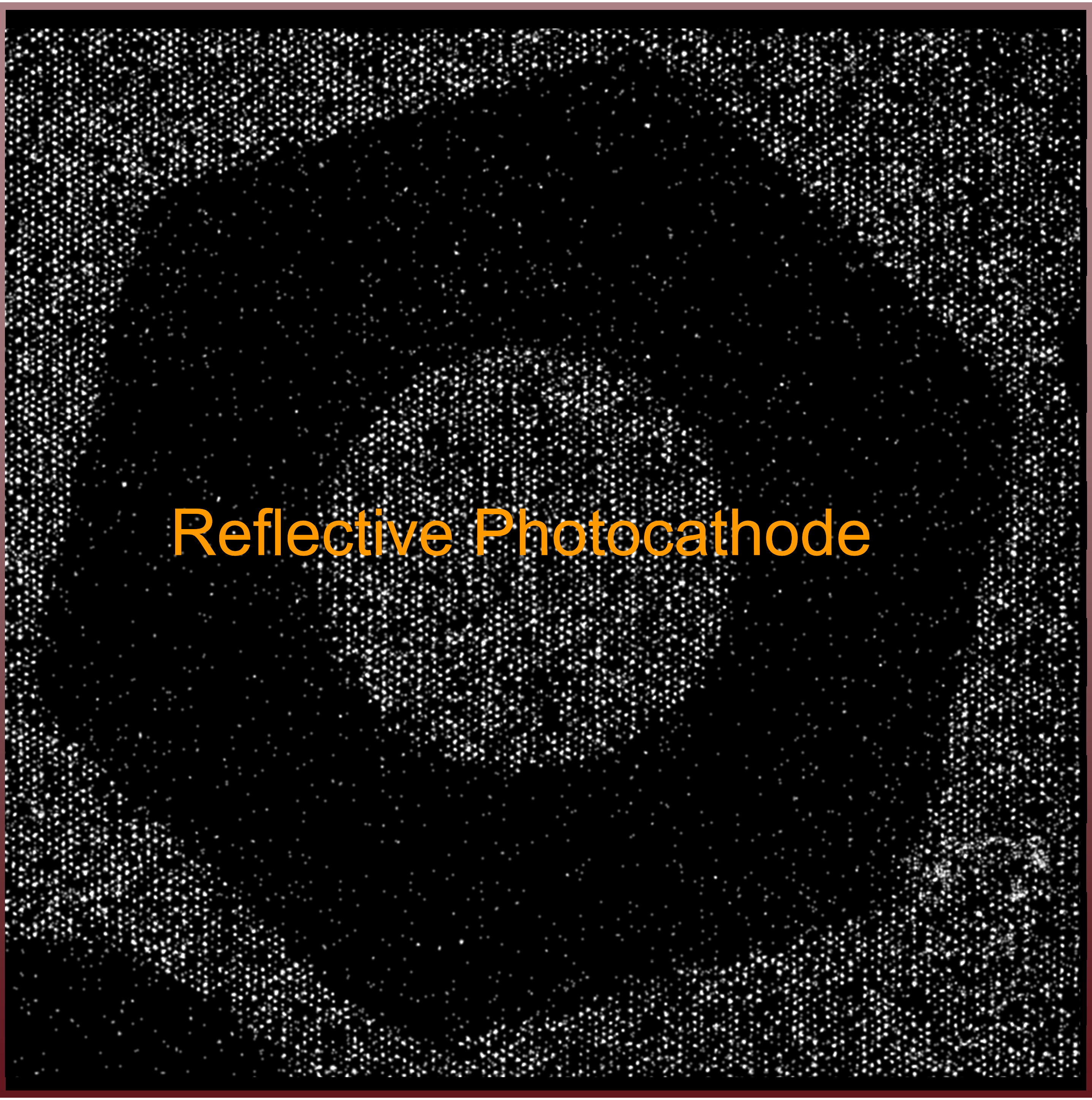
Reflective Photocathode

CIP

The use of Xpol as readout plane of a Micro Channel Plate coupled to a suitable photocathode in vacuum

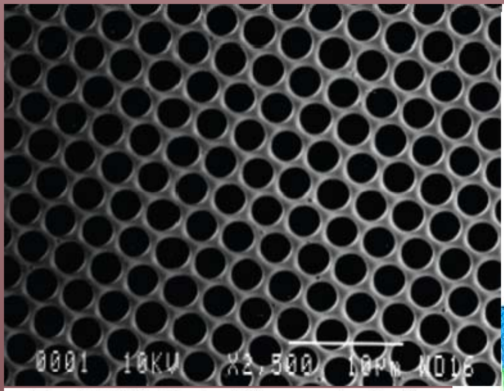

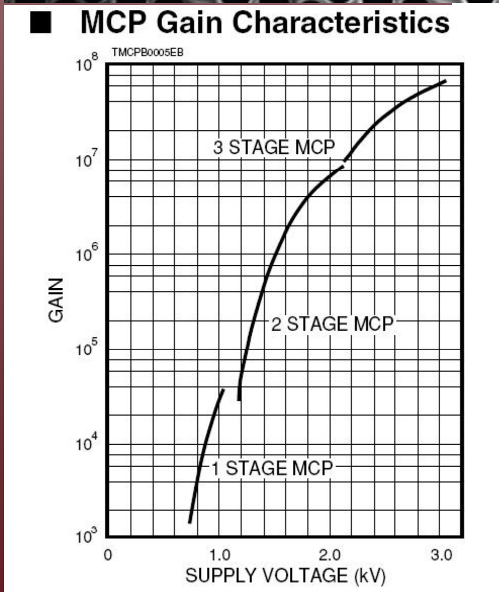

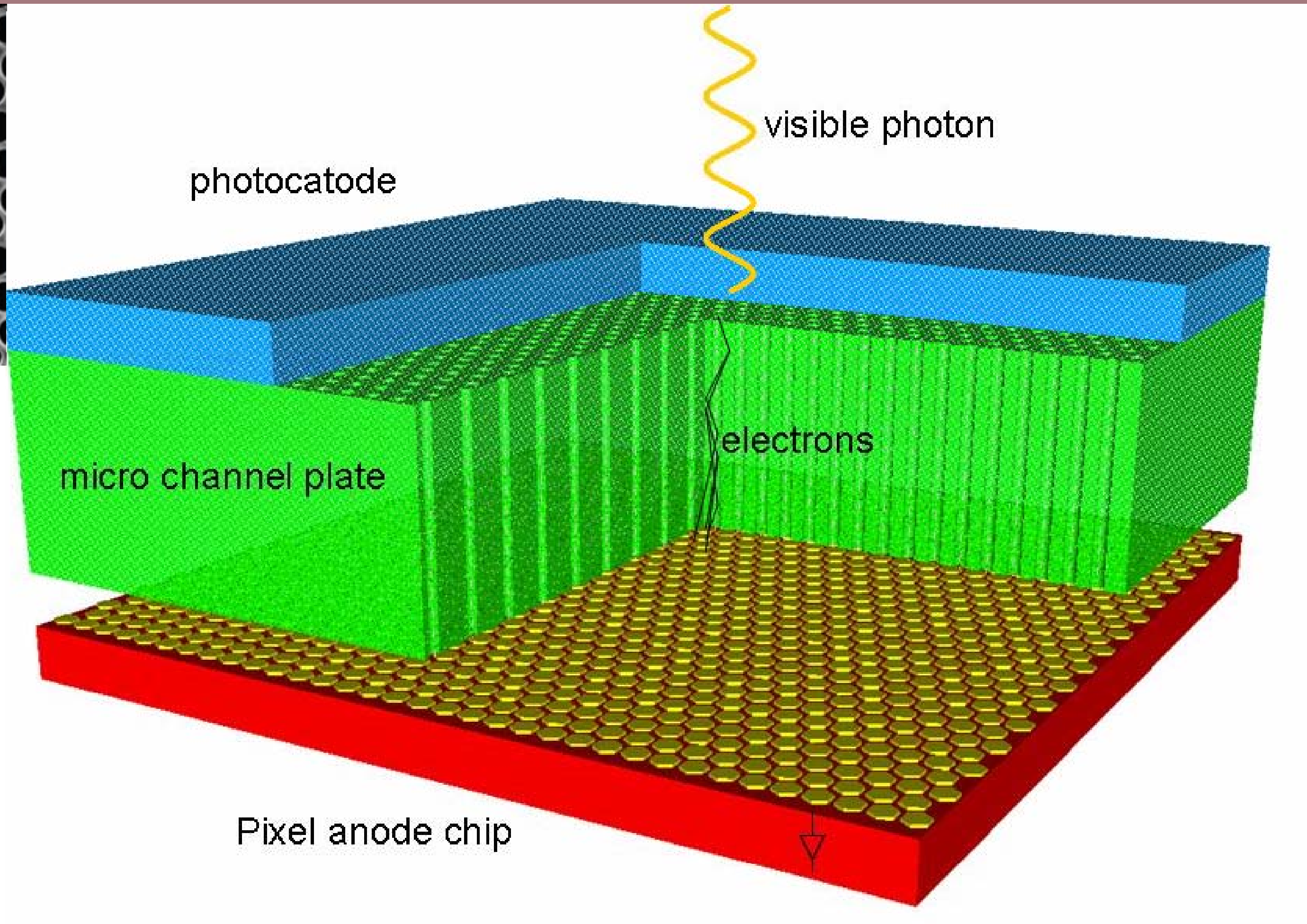

First test in collaboration with Space Science Laboratory, Berkeley

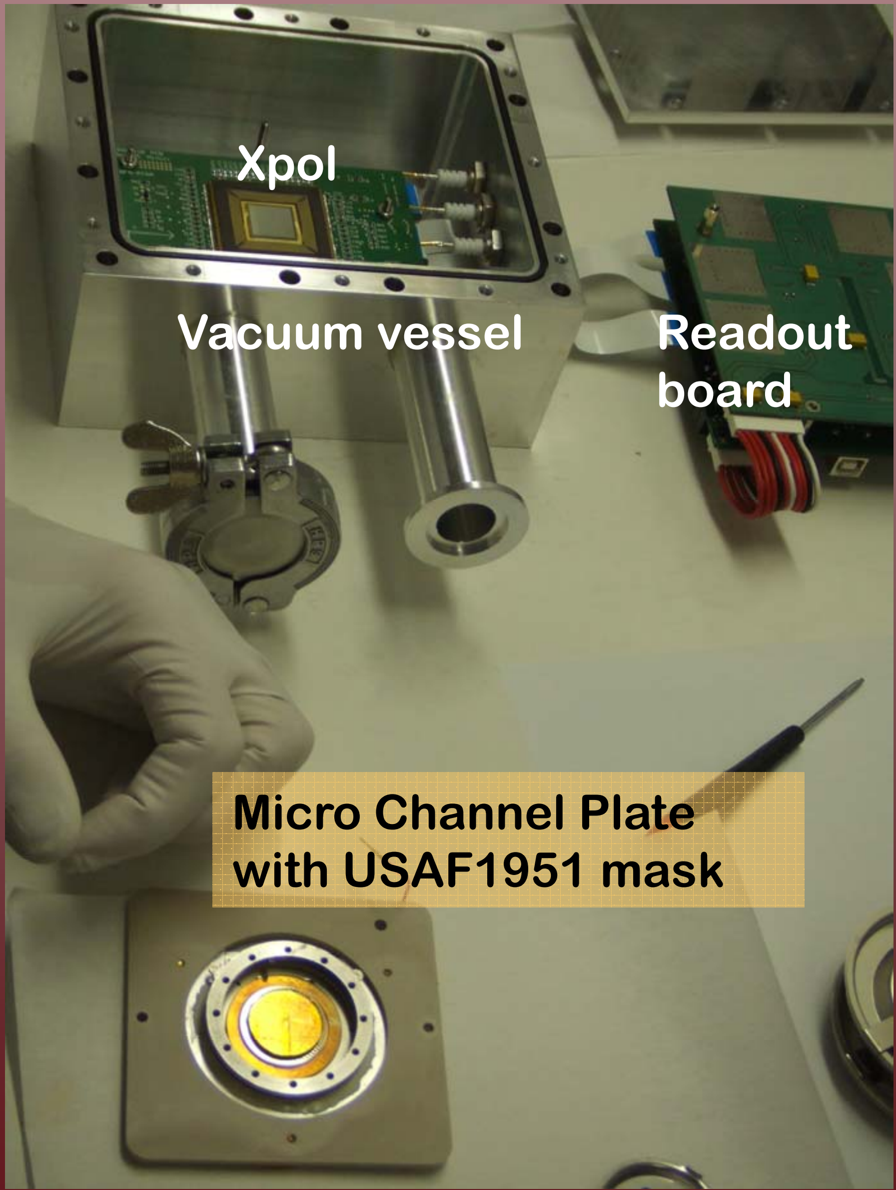

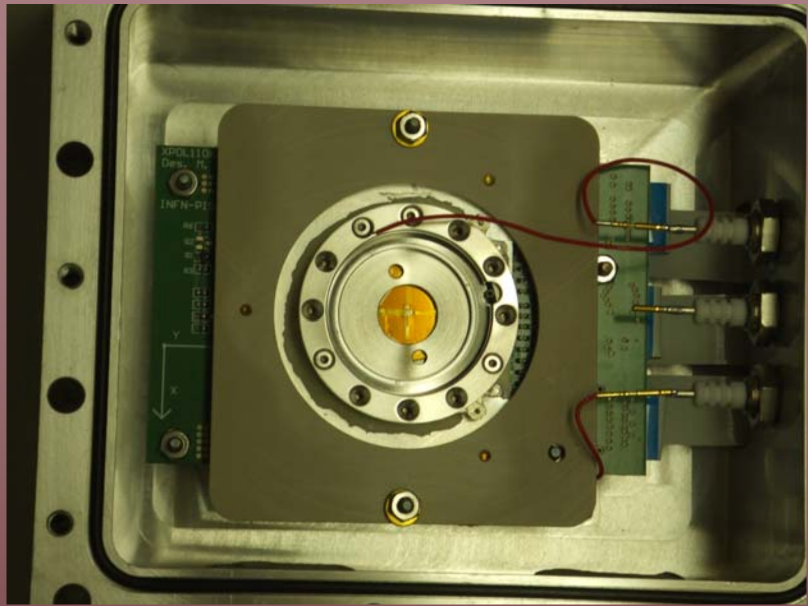

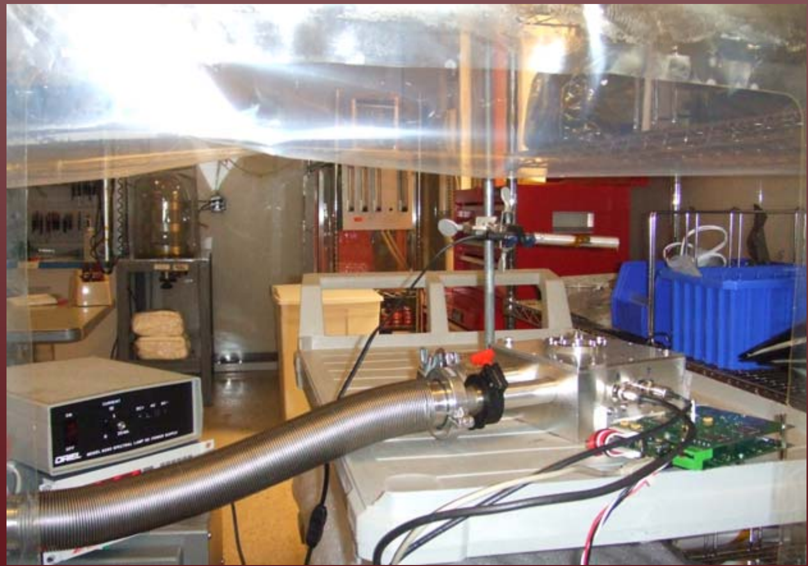

The events

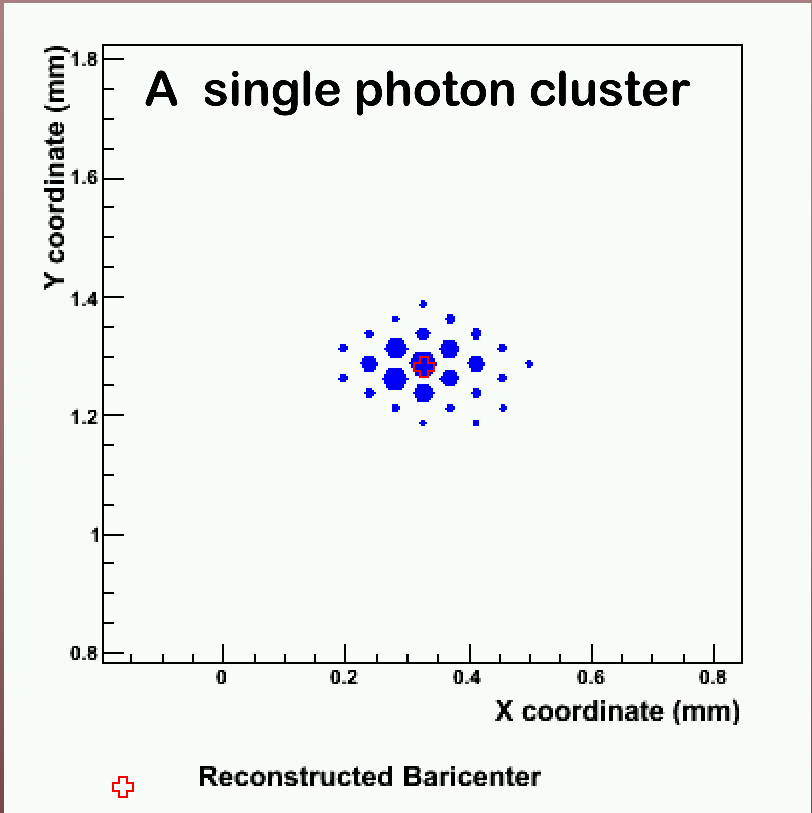

At low rate the detector records single photon events in window mode (<1K channels/frame, frame rate up to 10KHz).

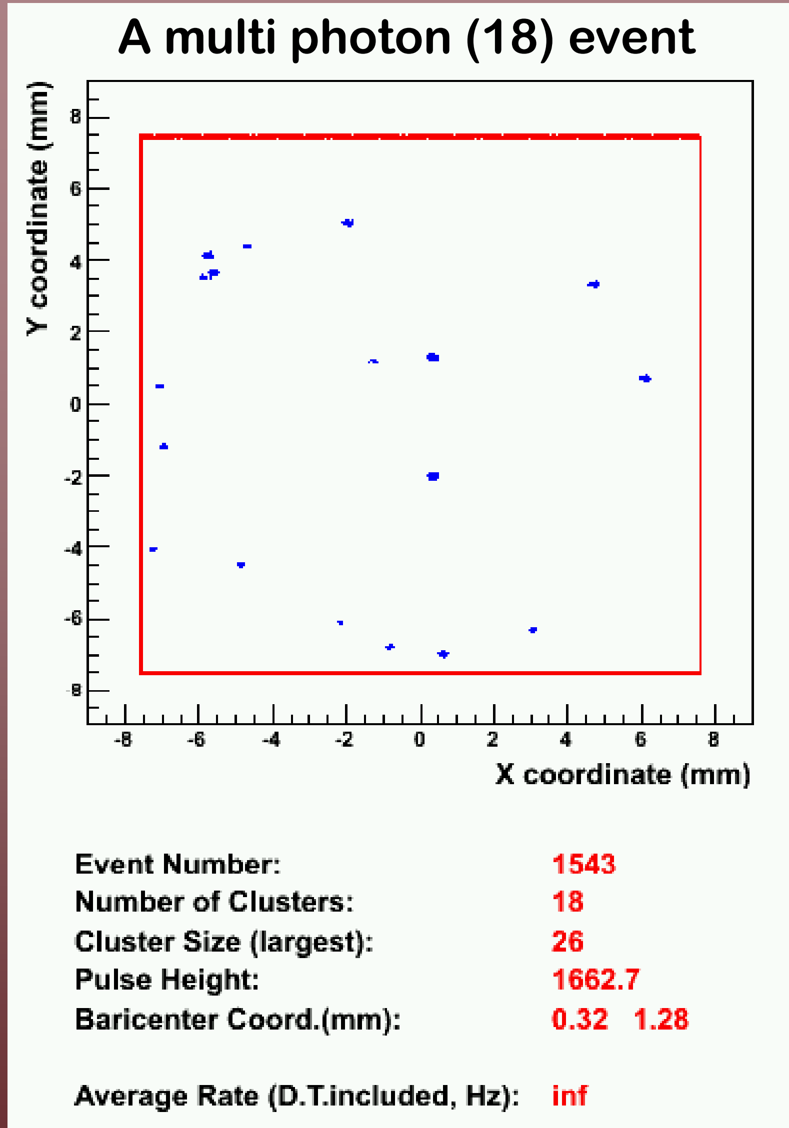

Thanks to the high granularity, at high rate the detector can resolve up to few hundreds of photons/frame in full frame readout mode (1KHz frame rate, up to ~200KHz photon rate)

The USAF1951 3-Bar Resolving Power Test Chart

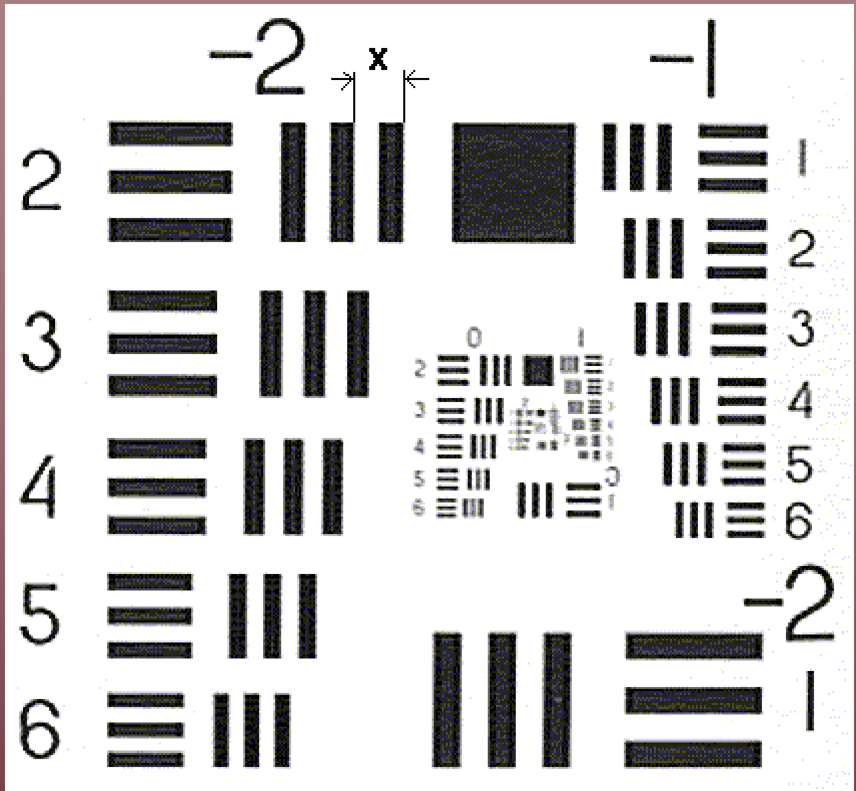

Line pairs/mm = $2^{n+(m-1)/6}$

X (mm) = $2^{-n-(m-1)/6}$

Es. n=6, m=1, $X=2^{-6}=1/64=15.6\mu m$

n=6, m=2, $X=2^{-(6+1/6)}=1/72=14\mu m$

n=6, m=6, $X=2^{-(6+5/6)}=1/114=8.7\mu m$

n=7, m=1, $X=2^{-7}=1/128=7.8\mu m$

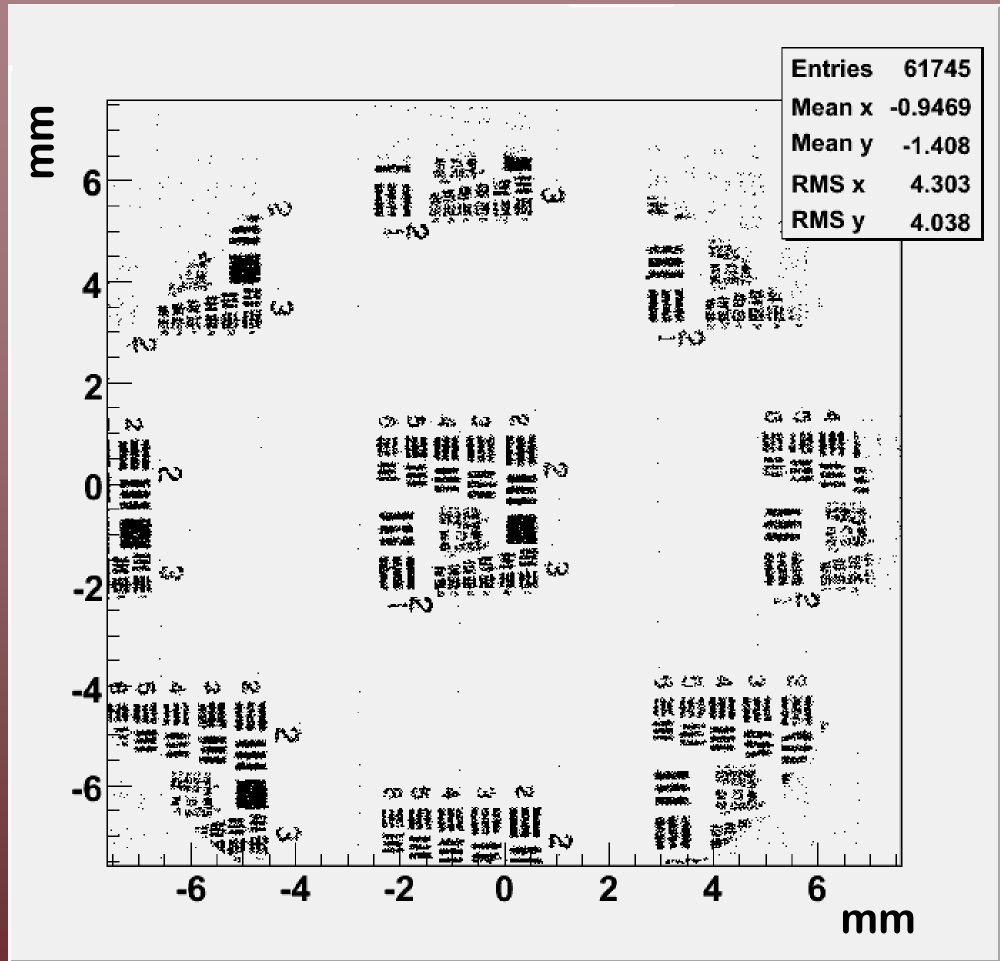

Full detector image

MCP 12.5mm aperture 15mm pitch

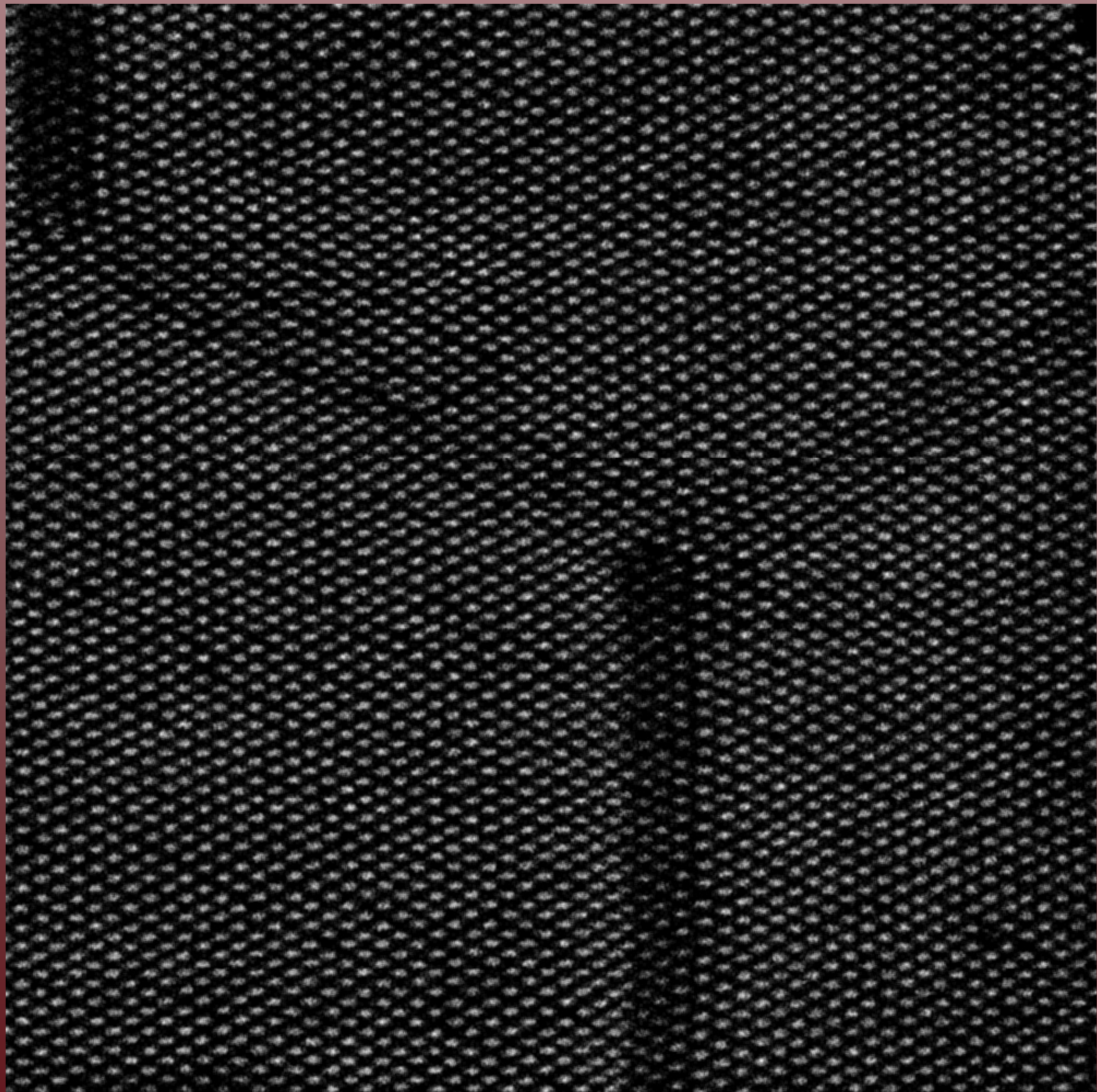

$1mm^2$ flat field image

MCP 10μm aperture 12μm pitch

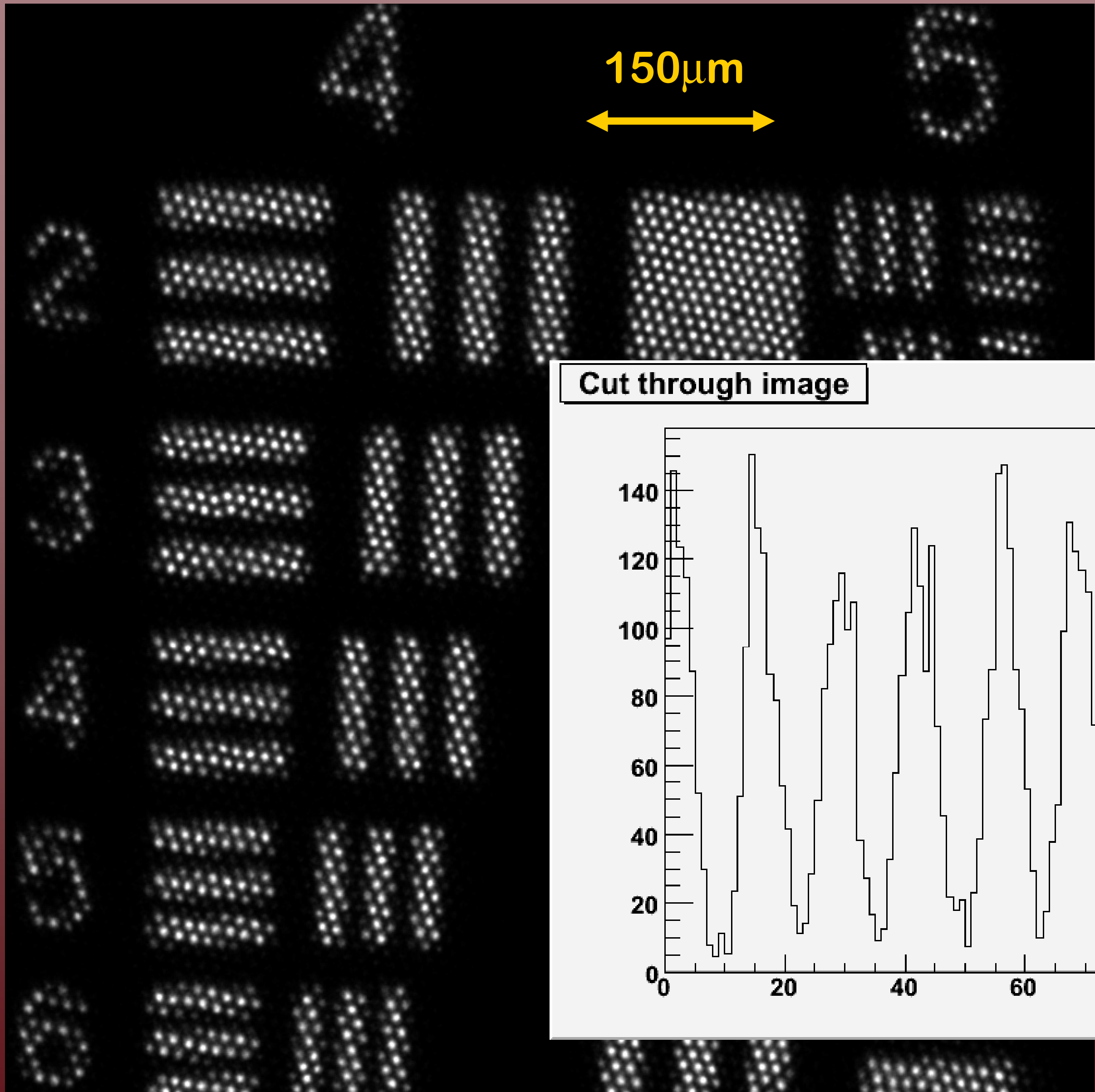

In a 140μm square easily resolved 150 spots.
The peak width includes the electron cloud width.

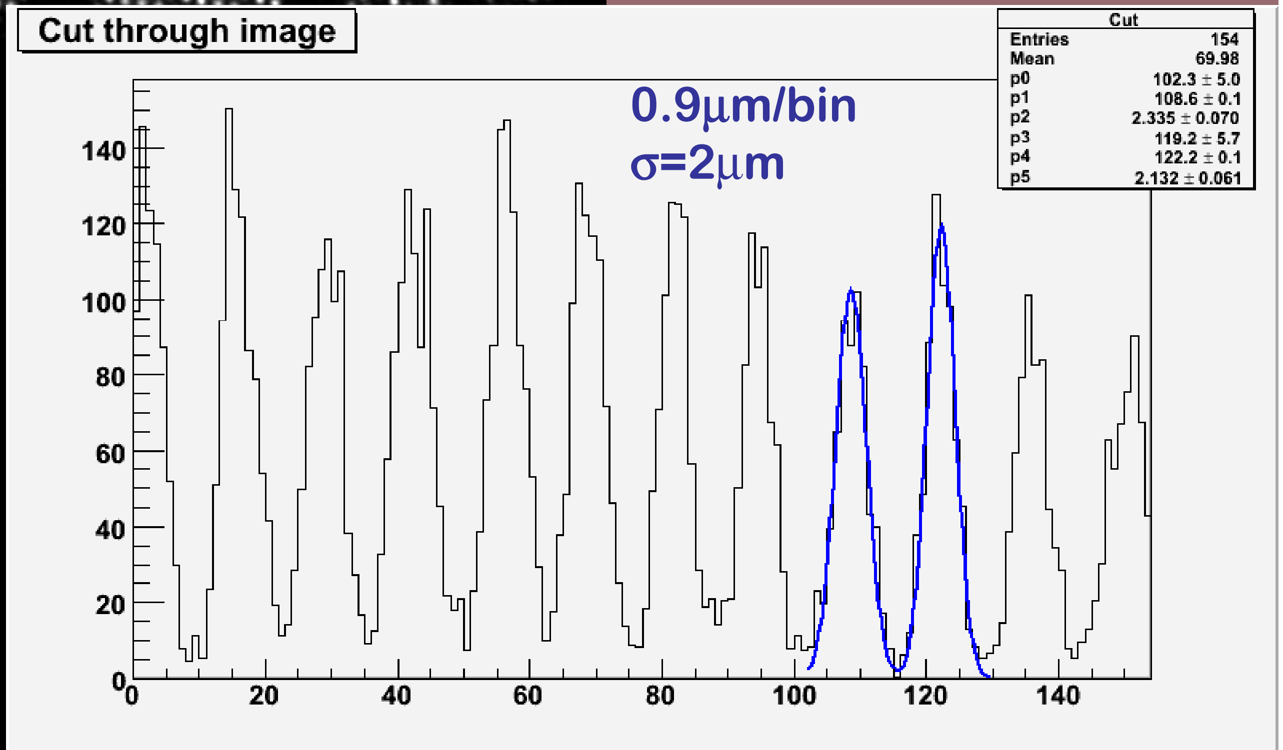

MCP 4μm aperture 5.5μm pitch

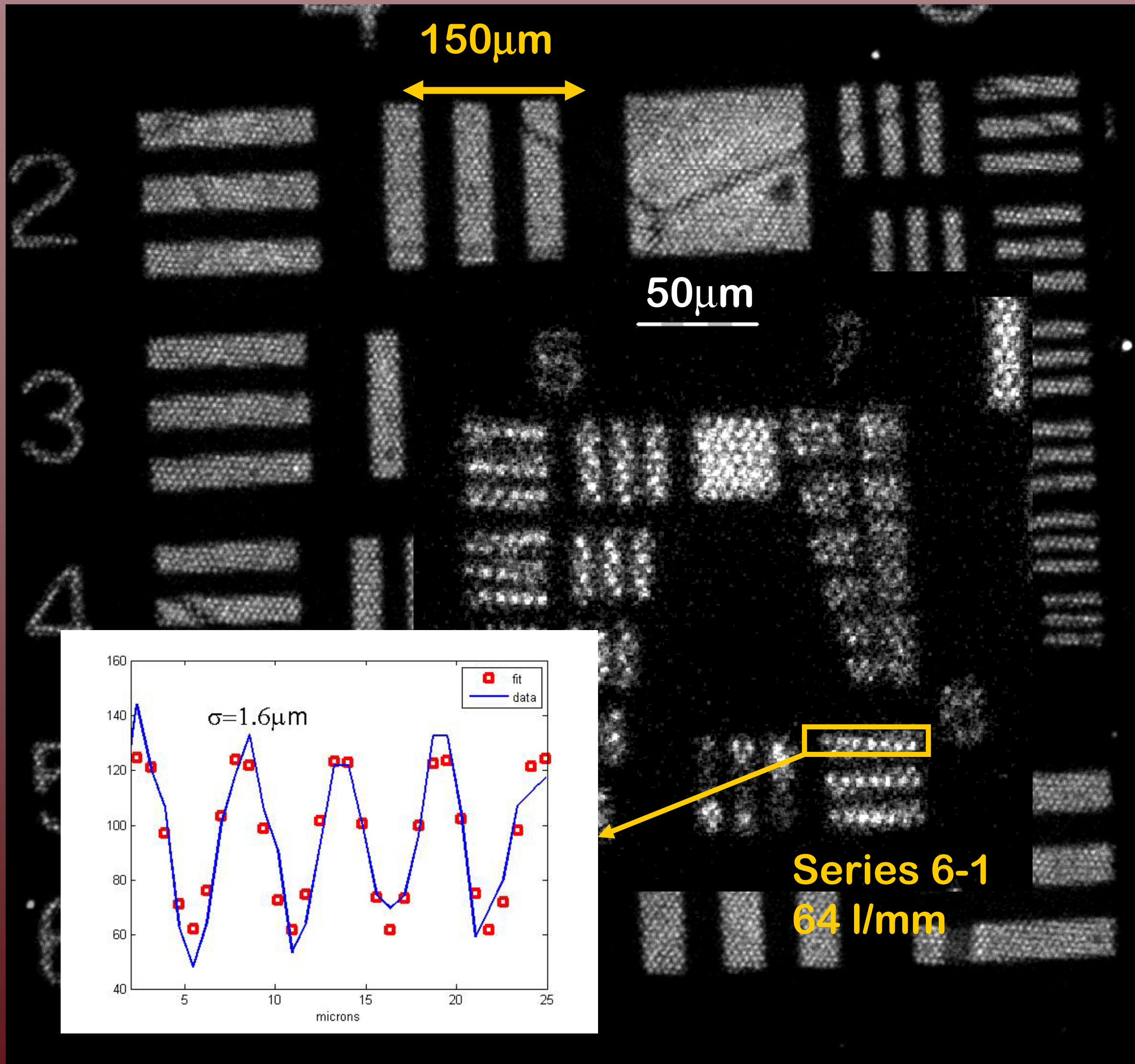

The MCP+ASIC as visible light single photon imaging photomultiplier

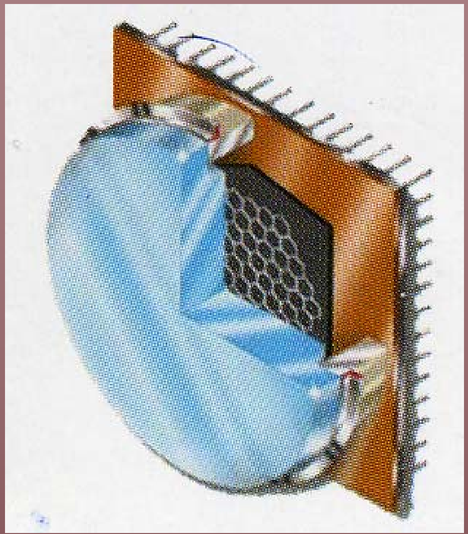

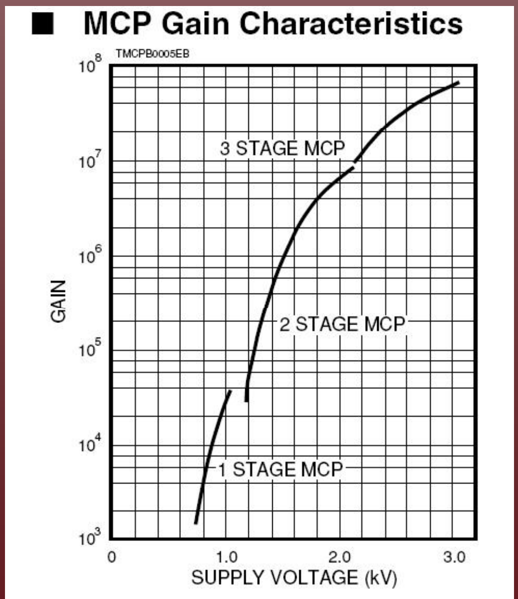

The existing electronic devices with the required pitch and number of pixels are the CCDs (integrating, i.e do not allow photon by photon processing).
Photon → photo-electron → 10^4 gain → phosphor screen → intensified light → CCD

With the CMOS pixel ASIC the chain is
Photon → photo-electron → 10^4 gain → ASIC

The actual Xpol chip is perfect for a detector with *enormous potentialities:*

- **ultra high resolution (2μm),**
- **100ps timing capability**
- **reasonably fast (10KHz),**
- **single photon counting (noiseless)**
- **imaging (300 X 352 pixels, 15mmX15mm)**

***Next step* → Pixie counting chip**

- **600x800 Pixels at 40μm pitch (25X30mm² area)**
- **parallel counting 1MHz/pixel, several GHz/chip**
- **5KHz Frame rate**
- **lower threshold**

applications

Molecular Imaging

Optical spectroscopy (prismatic). Actual devices use a unimimensional delay line readout with photocathode and MCP. Xpol can improve by orders of magnitude the resolution.

Mass spectroscopy: in this case there is no photocathode, the MCP is used directly as detector. The high Xpol spatial resolution allows very compact design.

Adaptive Optics: there is the need of a large detector (512X512 pixels) with μm resolution at high frame rate (>1KHz). SSL people propose 4 Medipix2 assembled together using the TOT function as ADC (pixel interpolation)

TimePix with "analog" (TOT) interpolation

(John Vallerga – 9th IWoRiD: Erlangen July 2007)

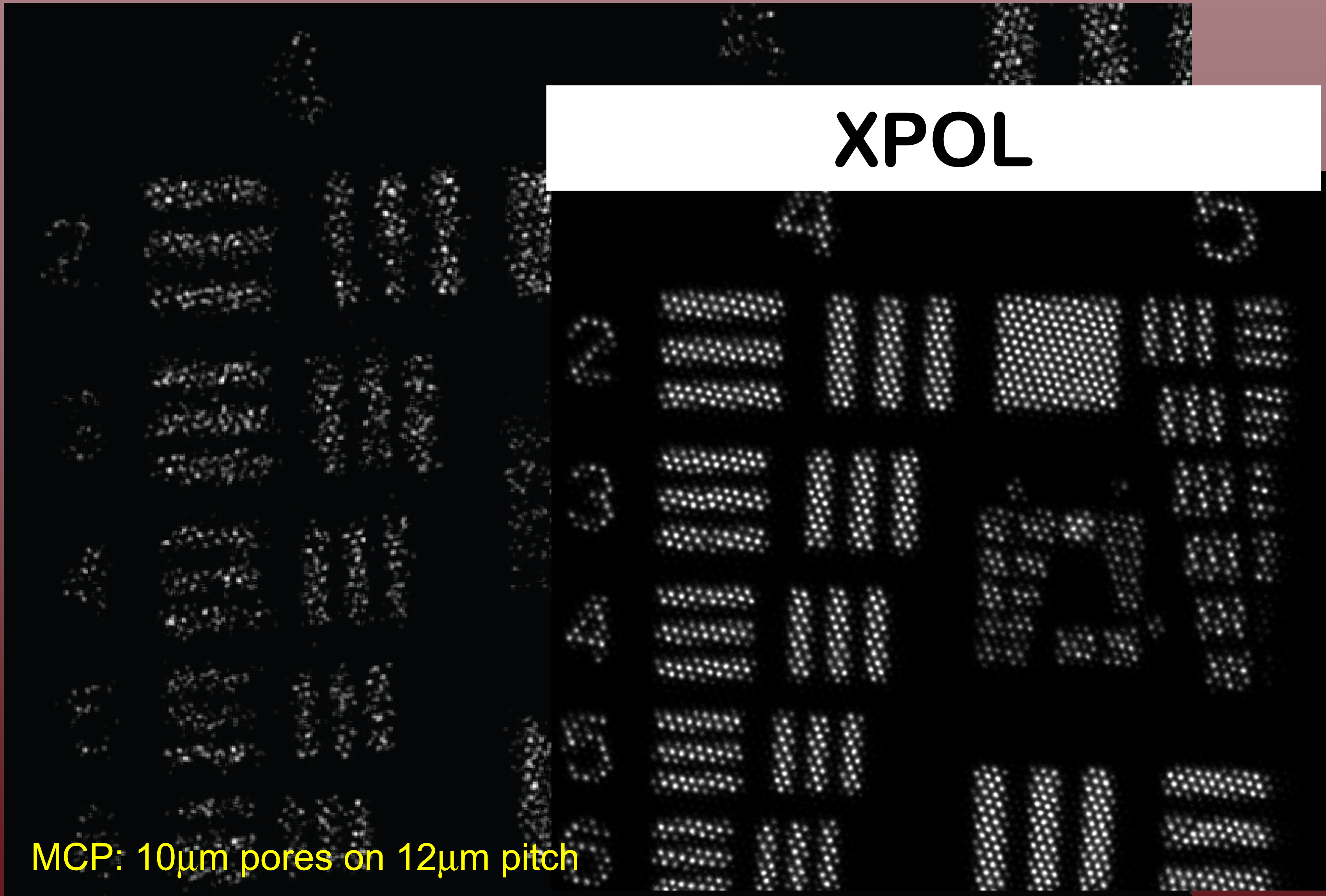

	Xpol	MEDIPIX2	PIXIE
Technology:	CMOS 0.18 μm	CMOS 0.25 μm	CMOS 0.18 μm
Type:	analog	digital (counting)	digital (counting+ ToT+Time stamp)
Area:	15x15=225mm^2(1.1X)	14x14=196mm^2(1X)	24x28=672mm^2(3.4X)
Pixel no.:	105.600 (1.6X)	65.536 (1X)	480.000 (7.3X)
Pixel density:	470/mm^2 (1.4X)	330/mm^2 (1X)	720/mm^2 (2.2X)
Pixel noise:	50 electrons *ENC*	110 electrons *ENC*	50 electrons *ENC*
Read-out scheme:	asynchronous, synchronous	synchronous	synchronous
Read-out trigger:	self-trigger, internal, external	internal, external	internal, external
Read-out mode:	single pixel, window, full frame (8-16 nodes)	full frame (1 node)	Full frame (up to 200 nodes)
Global threshold:	2000 el. (unadjusted)	1000 el. (adjusted)	200 el. (auto-adjusted)
Frame rate:	10 kHz	1 kHz	5 kHz
Event rate:	~10^5/s (10^2 ev. / frame)	~ 10^9/s	> 10^9/s
Resolution:	~ 1μm (analog int.)	~15μm (55/√12)	~11μm (38/√12)
Metal fraction:	90%	13%	47%

Conclusions

With devices like the ones presented the class of Gas Pixel Detectors has reached the level of integration, compactness and resolving power typical of solid state detectors. Depending on type of electron multiplier, pixel and die size, electronics shaping time, analog vs. digital read-out, counting vs. integrating mode, many applications can be envisaged for this class of detectors.

• A UV photo-detector with single electron sensitivity and excellent imaging capabilities has been shown. It is based on a semitransparent or reflective CsI photocathode followed by a Gas Electron Multiplier foil and by a large area, custom, analog, VLSI ASIC. The high granularity and low noise of the read-out plane allows to reconstruct with 4 μm resolution the centroid of the single electron avalanche. The detector position resolution is at the moment limited by the 50 μm pitch of the GEM foil.
Main problem ion is back-flow control; possible solutions exist and are under development.

• Sealed operation has been demonstrated with very good gain stability after more than 40 days of irradiation. Stability of performance after 1 year.

• A Ultra High Spatial Resolution Single Photon Counting Imaging Detector based on a MCP coupled to the 0.18μm CMOS Xpol ASIC (300 X 352 pixels, 15x15mm2). 4μm pores of the MCP were resolved indicating a ~1μm spatial resolution capabilty of the device. Good uniformity, high signal/noise ratio, stable operation conditions were achieved with different MCPs. Images in single photon readout mode (~10KHz) and multi-photon mode (up to ~200KHz) were acquired. Around 100 line pairs/mm can be resolved.